ROYAL ... ...MENT
L...DFC...D.

PROCUREMENT EXECUTIVE, MINISTRY OF DEFENCE

AERONAUTICAL RESEARCH COUNCIL

REPORTS AND MEMORANDA

The Steady Laminar Incompressible Boundary-Layer Problem as an Integral Equation in Crocco Variables: the Calculation of Non-Similar Flows

By R. D. Mills

Computing Department, Glasgow University

The Steady Laminar Incompressible Boundary-Layer Problem as an Integral Equation in Crocco Variables: the Calculation of Non-Similar Flows

By R. D. Mills

Computing Department, Glasgow University

Summary

The steady laminar incompressible boundary-layer problem in two dimensions has been posed as an integral equation in Crocco variables in the most general case and an algorithm developed for computing the similarity flows (Mills 1966).[10] The present report extends the algorithm to compute non-similar flows. Essentially it consists of replacing the x-derivative terms in the integral equation by finite differences so that the problem reduces to solving a non-linear integral equation across the boundary layer at successive x-stations starting from an initial solution at $x = 0$. To obtain convergence a double-field type of iteration with two relaxation factors has to be used. An analysis of the convergence of the process is given in the Appendix. The algorithm was found experimentally to be stable for every combination of step-sizes tried. A local matrix stability analysis of the algorithm is given in the Appendix.

A large number of examples have been computed, particularly flows with discontinuous suction distributions, periodic flows and separating flows. For the standard problems the results are in agreement with the known accurate computations. Some new problems are computed.

LIST OF CONTENTS

1. Introduction

In Ref. 10 Crocco's form of the steady two-dimensional laminar boundary-layer equation was converted into an integral equation in the most general case of arbitrary mainstream pressure distribution and arbitrary suction or blowing distributions at the wall. This is a generalisation of a well-known result for constant-pressure flow. In fact, it is the application of the Picard method for integrating ordinary differential equations to the non-linear parabolic partial differential equation of boundary-layer theory. Crocco's formulation of the boundary-layer problem is very well suited to this kind of conversion, though it can also be applied to other formulations.

The practical consequence of this work is the provision of an algorithm for numerical computation, as the integral equation can readily be solved on a digital computer by the method of successive approximation. The algorithm has been investigated for the similarity flows by the present author and extensive tables of the characteristics of these flows are given in Ref. 10. Cohen and Reshotko[2] had, unknown to the present author, used this algorithm for computing similarity solutions in compressible boundary-layer flow. The algorithm has also been successfully applied to the problem of the compressible and incompressible mixing of two parallel streams (*see* Ref. 12). This same idea had been used by Weyl[25] for computing some of the incompressible similarity flows. Weyl, however, used the Falkner–Skan form of the boundary-layer equation and this leads to an integral equation with exponential terms in its kernel, which is not so attractive computationally as the present formulation. Thus it seemed to the present author to be worth while to try to extend the algorithm to the general boundary-layer problem in view of its effectiveness for computing the similarity flows. Also, in a more general context, it would be an attempt to apply Picard's method for integrating ordinary differential equations to a well-known partial differential equation.

In the Picard algorithm the boundary conditions on either side of the boundary layer do not have to be satisfied explicitly; they are 'built-in' to the integral equation itself. This feature avoids the difficulties of solving a non-linear differential equation with 'two-point' boundary conditions, a problem usually overcome either by the so-called 'shooting' method (*see*, for example, Smith and Clutter[20]) or by solving iteratively a set of non-linear difference equations, often having an associated tridiagonal matrix of coefficients (*see*, for example, Fox, 3, p. 86). For the similarity flows, the Picard method leads to a non-linear integral equation for the shear stress as a function of the transverse velocity–ratio $u^* = u/U(x)$. For non-similar flows the method gives a non-linear integral equation for the shear stress as a function of u^* *and* x when the x-derivative terms are replaced by finite differences. This equation is then solved by iteration at successive x-stations from an initial solution at x_0. A preliminary Falkner–Skan-type transformation is used so that no special starting procedure is necessary when $x_0 = 0$, which can then correspond to a sharp leading edge or a stagnation point.

This plan for computing the boundary-layer equation seems straightforward and attractive. Several practical difficulties arise, however, in the numerical work. First, the Crocco boundary-layer equation possesses a singularity of the type $(1 - u^*)[\log \{(1 - u^*)^{-1}\}]^{\frac{1}{2}}$ at the outer edge of the boundary layer where $u^* = 1$. This difficulty is met by using a transformation of the independent variable which weakens the singularity (*see* Ref. 10). Secondly, there is the problem of the singularity at separation. The iteration process was found to converge extremely slowly if the separation point is approached by small x-steps. Consequently a special representation of the x-derivative terms was used to allow larger steps to be taken near separation. Also, in order to get very close to the separation point, it was found necessary to use a very small step-size *across* the boundary layer.

Thirdly, there is the problem of achieving *convergence*, and at a satisfactory rate, in the iterative process used to solve the integral equation. This problem was considered only superficially in Ref. 10 where it was found experimentally that 'under-relaxation' had to be used. As 'separation' conditions are approached the degree of under-relaxation has to be increased considerably to maintain convergence and ultimately the process fails, the same being true for large blowing rates. Generally, however, the iterative process can be made to converge by the use of a *single* relaxation factor ω.† Unfortunately for the non-similar flows, where a 'marching' procedure is now involved, a single-relaxation-factor process works only for one or two steps in the x-direction and then fails no matter how much ω is reduced. The author tried many artifices to overcome this problem, but without success. He eventually discovered a successful scheme which involves splitting the simple iteration process into two simultaneous processes with two relaxation factors ω and ω'. The author was led to this idea through working on the full Navier–Stokes equations (Ref. 13) and using the 'two-field' iteration technique of Thom.[22] Reasons for the failure of the simple scheme and the success of the double-field scheme are advanced in the Appendix, though they were not understood by the author when he first succeeded

---

† The relaxation factor is denoted by ω in this report to conform with the usual notation for such factors.

in getting the method to work. The basic iterative scheme was accelerated by the well-known Aitken technique and this frequently results in savings of over 25 per cent in the number of iterations. Another benefit of the accelerated scheme is that one can obtain convergence closer to the separation point than with the unaccelerated scheme.

Lastly, there is the problem of the *stability* of the marching process in the x-direction. It is well known that implicit difference methods for linear parabolic partial differential equations are unconditionally stable while explicit methods are conditionally stable. For non-linear problems it is necessary to consider *local* stability whereby the non-linear problem is *linearized* and the stability of the linearized problem taken to be representative locally of the stability of the full non-linear problem. The present difference representation of the boundary-layer problem is of implicit type and one would expect unconditional stability. The method was found experimentally to be stable for all the combinations of step-sizes in the streamwise and transverse directions that were tried. A local matrix stability analysis is given in the Appendix in support of this experimental evidence. In addition, a simple explicit-type scheme was tried and found to become rapidly unstable for every combination of step sizes used. A stability analysis of this scheme shows that instability will occur as x increases for any *fixed* combination of step sizes. This result is unfortunate since the explicit scheme avoids to a large extent the convergence difficulties of the implicit scheme.

2. Integral Equation Formulation of the Boundary-Layer Problem

Crocco's form of the laminar boundary-layer equation for steady incompressible two-dimensional flow is (*see*, for example, Ref. 18)

$$\frac{\partial^2 \tau}{\partial u^2} = \mu p'(x)\frac{\partial}{\partial u}\left(\frac{1}{\tau}\right) - \mu\rho\frac{\partial}{\partial x}\left(\frac{u}{\tau}\right) \tag{1}$$

with boundary conditions

$$\frac{\partial \tau}{\partial u} = \mu\frac{p'(x)}{\tau} - \rho w_s \quad \text{at } u = 0 \tag{2}$$

and

$$\tau = 0 \qquad \text{at } u = U(x), \tag{3}$$

where τ is the shear stress, u the velocity component in the x-direction, μ and ρ the coefficient of viscosity and the density of the fluid, w_s the velocity normal to the wall at $u = 0$ and $p'(x) = -\rho U dU/dx$ the pressure gradient corresponding to the external velocity $U(x)$. By two successive integrations which incorporate the boundary conditions, the boundary-value problem equations (1) to (3) can be converted into the integral equation (*see* Ref. 10)

$$\tau(u, x) = \int_0^{U(x)} \mu\left[\rho(U - u)\frac{\partial}{\partial x}\left(\frac{u}{\tau}\right) - \frac{p'(x)}{\tau}\right]du + \mu\rho(U - u)\int_0^u \frac{\partial}{\partial x}\left(\frac{u}{\tau}\right)du - \rho w_s(u - U). \tag{4\dagger}$$

This equation is a generalisation of Crocco's result for constant pressure. In a wider sense it is an application of Picard's idea to a partial differential equation.

The shear stress τ is now given the form

$$\tau = \frac{\mu U^{\frac{3}{2}}(x)}{\sqrt{(2xv)}}G(u^*, x), \tag{5}$$

---

† Strictly speaking, (4) should be termed an *integro-differential equation*. However, as it reduces to an integral equation for the similarity flows and also when the $\partial/\partial x$ terms are replaced by differences in the present treatment of the non-similar flows, the term *integral equation* will be retained.

4

where

$$u^* = u/U(x) \tag{6}$$

and $v = \mu/\rho$ is the kinematic viscosity coefficient of the fluid. This preliminary Falkner–Skan-type transformation removes the awkward leading-edge singularity from the formulation of the problem. (Note that the normalisation with respect to x has been altered from the more general type used in Ref. 10 as the latter is not so convenient for non-similar problems. In fact, if the length $g(x)$ in Ref. 10 is replaced by $\sqrt{(2vx/U)}$ then the shear stress function $F(u^*)$ of Ref. 10 becomes identical with the above $(G(u^*))$. The class of 'similarity' flows has external velocity distributions $U(x)$ and suction or blowing velocity distributions $w_s(x)$ such that G becomes a function of u^* only.

Substitution of (5) and (6) into (4) leads to the following integral equation for $G(x, u^*)$:

$$G(u^*, x) = \int_{u^*}^{1} \left[\frac{2P + (1 + P)u^* - (1 + 3P)u^{*2}}{G} + 2(u^* - u^{*2})x\frac{\partial}{\partial x}\left(\frac{1}{G}\right) \right] du^*$$

$$+ (1 - u^*)\int_{0}^{u^*} \left[\frac{(1 + P)u^*}{G} + 2u^* x\frac{\partial}{\partial x}\left(\frac{1}{G}\right) \right] du^* + W(x)(1 - u^*), \tag{7}$$

where

$$P(x) = \frac{x}{U}\frac{dU}{dx} \quad \text{and} \quad W(x) = w_s(x)\sqrt{\left(\frac{2x}{vU}\right)}. \tag{8}$$

2.1. Weakening the Singularities

It was shown in Ref. 10 that improved numerical results can be obtained for the similarity flows if we make the change of independent variable u^* to s where

$$1 - u^* = s^2. \tag{9}$$

The reason is simply that the function $G(s)$ is *less singular* than $G(u^*)$ at the outer edge of the boundary layer. A similar improvement can generally be anticipated for non-similar flows when the integral equation (7) is transformed to

$$G(s, x) = \int_{0}^{s} \left[\frac{2(1 + 5P)s^3 - 2(1 + 3P)s^5}{G} + 4(s^3 - s^5)x\frac{\partial}{\partial x}\left(\frac{1}{G}\right) \right] ds$$

$$+ s^2 \int_{s}^{1} \left[\frac{2(1 + P)(s - s^3)}{G} + 4(s - s^3)x\frac{\partial}{\partial x}\left(\frac{1}{G}\right) \right] ds + W(x)s^2 \tag{10}$$

with the aid of (9). The numerical solution of this equation is the main concern of this report.

Near the separation point x_s the shear stress τ is reckoned to behave like $(x_s - x)^{\frac{1}{2}}$ and so the usual finite-difference formulae for $\partial(1/\tau)/\partial x$ become increasingly inaccurate as $x \to x_s$. This difficulty can be mitigated by using differences based on τ^2 (or equivalently on G^2 in equation (10)) rather than on $(1/\tau)$. Thus we write the x-derivative term in (10) as

$$\frac{\partial}{\partial x}\left(\frac{1}{G}\right) = -\frac{0.5}{G^3}\frac{\partial G^2}{\partial x} \tag{11}$$

and base our differences on G^2 which is less singular in the neighbourhood of $x = x_s$. Greater accuracy is then obtainable near separation for a given step-size δx (see Table 1). This is particularly important in the present work, for the iterative process is very slow to converge if very small values of δx are used in approaching the separation point. Furthermore, it is expected that by the use of (11) some improvement in accuracy should result in the neighbourhood of step discontinuities of suction, for an algebraic singularity is known to occur in τ at these discontinuities (see Refs. 17 and 14). The papers of Gadd[4] and Schönauer[19] should be consulted for other methods of treating these singularities.

5

Finally, it should be observed that for computational purposes the above formulation of the boundary-layer problem has the valuable property which is independent of the external velocity distribution $U(x)$: the domain of the solution is the rectangular region $0 \leqslant s \leqslant 1, x \geqslant 0$ (Fig. 1), so that it is not necessary to adjust the step-size across the boundary layer when the latter changes appreciably in thickness. Also, no special starting procedure is necessary; one simply sets $x = 0$ in equation (10) and solves the resulting integral equation. This step is built in naturally as the first step in the complete computation.

2.2. Boundary-Layer Characteristics

In the present formulation of the boundary-layer problem the local coefficient of skin friction $c_f = 2\tau_w/\rho U^2$ is given by the relation

$$c_f \left(\frac{Ux}{2\nu} \right)^{\frac{1}{2}} = G(1, x), \tag{12}$$

while the coordinate z normal to the wall is given by

$$z \left(\frac{U}{2\nu x} \right)^{\frac{1}{2}} = \int_s^1 \frac{2s}{G(s, x)} ds \tag{13}$$

and the displacement thickness δ_1, momentum thickness δ_2 and energy thickness δ_3 of the boundary layer take the forms

$$\delta_1 \left(\frac{U}{2\nu x} \right)^{\frac{1}{2}} = \int_0^1 \frac{2s^3}{G(s, x)} ds, \tag{14}$$

$$\delta_2 \left(\frac{U}{2\nu x} \right)^{\frac{1}{2}} = \int_0^1 \frac{2(1 - s^2)s^3}{G(s, x)} ds, \tag{15}$$

and

$$\delta_3 \left(\frac{U}{2\nu x} \right)^{\frac{1}{2}} = \int_0^1 \frac{2(1 - s^2)(2s^3 - s^5)}{G(s, x)} ds \tag{16}$$

respectively.

3. Method of Solution of the Integral Equation

The basic idea of the present method is to replace the x-derivative terms by finite differences and solve the resulting integral equation in s across the boundary layer by the method of successive approximation. Once the solution is obtained at an initial station $x = x_0$ (usually 0) it is advanced by a marching procedure to $x_0 + \delta x, x_0 + 2\delta x$ and so on. This idea is related to the method of Hartree and Womersley[5] and applied by Smith and his co-workers[20] to boundary-layer problems. Whereas these authors solve a differential equation across the boundary layer, the present author solves an integral equation.

The x-derivative terms in equation (10) are transformed to the form (11) and the following Lagrangian three-point formula used

$$\frac{\partial G^2}{\partial x}(s, x) = \frac{1}{2\delta x} \left(3G^2(s, x) - 4G^2(s, x - \delta x) + G^2(s, x - 2\delta x) \right) \tag{17}$$

where δx is the step-length in the x-direction. As remarked earlier the initial solution presents no special difficulty, for (10) reduces to an 'ordinary' integral equation when $x = 0$. At the first x-station it is necessary to use the two-point formula

$$\frac{\partial G^2}{\partial x}(s, x) = \frac{1}{\delta x} \left(G^2(s, x) - G^2(s, x - \delta x) \right) \tag{18}$$

6

since the solution is known at only one preceding x-station. Thereafter, equation (17) is used. These formulae have truncation errors of order δx for the first step and $(\delta x)^2$ for every subsequent step. (It would be possible to have an error of order $(\delta x)^2$ throughout by using the difference formula

$$\frac{\partial G^2}{\partial x}(s, x) = \frac{2}{\delta x}\left(G^2(s, x) - G^2(s, x - \delta x)\right) - \frac{\partial G^2}{\partial x}(s, x - \delta x) + O((\delta x)^2), \tag{19}$$

for the first step, since it can then be taken with an error of order $(\delta x)^2$ after setting up and solving the appropriate integral equation for $\partial G(s, 0)/\partial x$. Gadd's[4] paper illustrates the application of this idea to the differential form of the boundary-layer problem.)

3.1. Solution Technique

The following simple functional iteration scheme was found to *converge* satisfactorily for the similarity flows (see Ref. 10):

$$G^{(n+1)}(s) = \omega\phi(G^{(n)}(s)) + (1 - \omega)G^{(n)}(s), \tag{20}$$

where ω is a suitably chosen relaxation factor, ϕ is the right hand side of equation (10) and n is the iteration index. The scheme is actually used in a *discretized* form on replacing the integrals in ϕ by some quadrature formula. In fact, the integrals were computed using Simpson's rule. This requires the use of interpolation after each cycle of iteration to give the solution at the intermediate nodes. The technique is as described in detail in Ref. 10, with the following slight modification. Instead of 'stopping short' of the singularity, say at $s = 10^{-10}$, s was taken as exactly zero and the integrands at $s = 0$ in equation (10) were both set to zero. The first integrand is in fact zero and though the second is infinite the integral at $s = 0$ is multiplied by s^2 and the limiting value is zero by the boundary condition. To check this procedure the integration from $s = 0$ to $s = 2\delta s$ was performed by a Radau-type quadrature formula (Ref. 7, p. 338) which avoids using the values of the integrands at $s = 0$. In the cases tested, the results for a given value of δs were no better than those obtained by the present technique. The latter was thus preferred, not only for this reason, but also because using a second quadrature formula of the Radau type requires further interpolation and all this involves many extra programming instructions in the inner loop of the program.

When applied to the (non-similar) equation (10) the iterative scheme equation (20) converges at the initial station $x = 0$. For $x > 0$, equation (20) converges only for one or two steps and then only after many iterations with very small value of ω; thereafter it always fails to converge. The explanation for this failure is given in the Appendix. The following iterative scheme, involving two suitably chosen relaxation factors ω and ω', was found to produce convergence:

$$\left.\begin{aligned}
F^{(0)}(s, x) &= 0 \\
G^{(n+1)}(s, x) &= \omega\Phi(G^{(n)}(s, x), F^{(n)}(s, x)) + (1 - \omega)G^{(n)}(s, x) \\
F^{(n+1)}(s, x) &= \omega'\chi(G^{(n+1)}(s, x)) + (1 - \omega')F^{(n)}(s, x)
\end{aligned}\right\}, \tag{21}$$

where Φ is the right hand side of equation (10) and χ is given by

$$\chi = x\frac{\partial}{\partial x}\left(\frac{1}{G(s, x)}\right). \tag{22}$$

The 'single-field' process for G has in effect been replaced by a 'double-field' process for G and the x-derivative term F. This scheme is again actually implemented in the discretized form obtained by replacing the integrals in Φ by Simpson's rule and the derivative in equation (22) by the difference equations (17) or (18).

To start with, ω and ω' are given relatively high values, usually $\omega = \omega' \approx 0.3$ to 0.5. At $x = 0$ the initial approximation to the solution was taken simply as $G^{(0)}(s, 0) = s^2$. For succeeding steps in the x-direction, the initial approximation $G^{(0)}(s, x)$ was taken as the final (fully-iterated) solution $G(s, x - \delta x)$ at the previous x-station. This is generally a very good initial approximation except in regions where the solution changes very rapidly with x. The convergence criterion was based on the sum of the absolute values of the differences of the elements of two successive vectors of iterates being less than a prescribed value, usually 10^{-6}. If as x is increased convergence does not take place at all (as indicated by a rapid increase in the wall shear stress as

the iterations proceed) then ω and ω' are both reduced, usually by about 10 per cent, and the process started afresh. When making changes in the step-size δx, a good working rule for the determination of new values of ω and ω' was found to be

$$\omega\omega'\frac{x}{\delta x} = \text{const.} \approx 3 \text{ to } 5 \qquad (23)$$

(this parameter arises in the double-field iteration matrix, *see* Appendix).

This algorithm was tested for a very wide range of mesh sizes δx and δs. In every case convergence was obtained with appropriate positive values of ω and ω' (except very near to separation, *see* Appendix) and the algorithm was stable on marching in the x-direction.

The iteration process described above was accelerated by the well-known Aitken technique. A new sequence of iterates $\{G'^{(n)}(s, x)\}$ is formed from

$$G'^{(n)} = G^{(n)} - \frac{(G^{(n+1)} - G^{(n)})^2}{G^{(n+2)} - 2G^{(n+1)} + G^{(n)}}, \qquad (24)$$

where $G^{(n)}$, $G^{(n+1)}$ and $G^{(n+2)}$ are three successive iterates of the 'old' sequence $\{G^{(n)}(s, x)\}$. Note that this is simply the Aitken process applied to each individual component of the vector $\mathbf{G}(x)$, and not the generalised Aitken process involving a vector acceleration as described for example in Ref. 6, p. 115. The latter process could well give more rapid convergence per acceleration but this must be weighed against the time required to effect the matrix inversion needed at each acceleration. The former technique gives a worthwhile saving in computer time, for the number of iterations required to give a prescribed degree of convergence can be reduced by more than 25 per cent particularly near separation. The accelerated process also has the advantage that on approaching separation it usually converges at a few x-stations beyond the point where the unaccelerated process fails.

The accuracy of the computation across the boundary layer has been investigated in detail in Ref. 10 for the similarity flows. These results can be expected to give a guide as to what accuracy can be expected for a given subdivision δs across the boundary layer in the non-similar flows, but clearly the accuracy depends also on the subdivision δx in the x-direction. In regions of gradual change in pressure gradient, or suction at the wall, it is possible to use relatively large values of δx. In regions of rapid or discontinuous change it is necessary to use small values of δx. In the case of flows with separation, it was found that for fixed δx the smaller the value of δs, the closer one can get to, and compute accurately the position of, the separation point. The reason for this phenomenon is given in the Appendix.

4. Examples

4.1. Discontinuous Boundary-Layer Flows

The method was first applied to flows having discontinuous suction or blowing at the wall. Fig. 2 shows the variation of the wall skin friction for a flat plate having uniform suction $S = -(w_0/U_\infty)(U_\infty l/v)^{\frac{1}{2}} = 1.5$ applied downstream of an initial impermeable portion. Small values of δx were used in the immediate vicinity of the step change. The results agree with those of Refs. 17 and 20. The suction 'pulse' considered by Rheinboldt was also computed and the results are contained in Fig. 2. Just downstream of the pulse the present results differ slightly from Rheinboldt's. Smith and Clutter found the same deviation and believed their results to be in error in this region. It would thus seem that in reality Rheinboldt's solution is slightly in error just aft of the pulse. Fig. 2 also contains for comparison an approximate analytical solution given in a paper[14] by the present author. In addition, this paper contains a comparison between the analytical and numerical solutions for a pulse with $S = 0.5$.

Fig. 3 depicts the effect of concentrating the same total quantity of suction into a narrower and narrower slot. Each pulse width was divided into 20 steps and the appropriate value of δx retained for about one pulse width downstream. In these three cases the disturbance introduced dies out in a distance that is relatively independent of how the suction is applied. The case of two spaced suction pulses with the same total suction quantity is shown in Fig. 4. This configuration appears to perturb the flow rather more than a single suction pulse with the same total suction quantity. Also shown in Fig. 4 are results for a single suction pulse followed by an equal blowing pulse, this arrangement giving zero net mass transfer at the wall. Fig. 5 gives the results for

a suction pulse starting at $x = 1.0$ of width 0.15 and $S = 1.5$ applied to three similarity flows. These correspond to the flat plate ($P = 0$), a wedge of 45 degrees semi-angle ($P = \frac{1}{3}$) and a forward stagnation point ($P = 1$). The results are all qualitatively similar but the thinning effect is less pronounced the larger the pressure gradient.

The effect on the wall shear stress of a step-change in the applied pressure gradient is shown in Fig. 6. It is important to know the response to such changes in assessing the merits of calculating boundary-layer flows by piece-wise joining of similarity solutions. The response is in fact relatively slow in the cases considered. These results agree with those of Smith and Clutter.[20]

It has been shown that though abrupt the changes in shear stress at the discontinuities are in reality continuous (Refs. 17, 10 and 14). Consequently, in all the above cases the following method of treating the discontinuities numerically was adopted. The discontinuity was not 'straddled' but was retained as a nodal point in the mesh. The step-size δx was reduced immediately on proceeding downstream from the discontinuity and the two-point formula, equation (18), was used for the first step. This procedure is necessary in any case if δx is changed at the step. If δx were not changed the three-point formula would give a doubtful estimate of the derivative because of the discontinuous change in slope at its 'middle' node.

4.2. Periodic Boundary-Layer Flows

Fig. 7 shows the effect of a periodic normal velocity at the surface of a flat plate. The flow quickly responds, with the displacement thickness lagging very slightly in phase behind the applied fluctuating velocity, while the wall shear stress remains almost exactly out of phase with the displacement thickness.

The effects on the flat plate flow of a periodic component $\varepsilon \sin (5\pi x/l)$ in the mainstream are shown in Fig. 6 for $\varepsilon = 0.01$ and 0.02. In the first case the flow is non-separating, at least as far as $x = 2.0$, having settled down with the shear stress taking a very slight phase *lead* over the fluctuating mainstream velocity and the displacement thickness remaining almost exactly out of phase with the wall shear stress. It is interesting to compare this phenomenon with the phase lead that occurs in *time*-fluctuating boundary layers and which is attributed physically to the relatively greater effect of the fluctuating pressure gradient on the slowly-moving fluid near the wall than on the faster-moving fluid at the outer edge of the boundary layer. When $\varepsilon = 0.02$, separation occurs just short of $2\frac{1}{2}$ cycles at $x = 0.996$. The tendency of the flow to separate at the given 'frequency' is rather marked considering the very small amplitude of the fluctuating component; this again resembles the time-periodic phenomenon.

4.3. Flows with Separation

The boundary layer corresponding to the potential flow $U = 2U_\infty \sin (x/a)$ about a circular cylinder of radius a in a stream of velocity U_∞ at infinity was next computed. Numerical details of the solution are given in Table 1 alongside the results obtained by Terrill.[21] As noted earlier it is difficult to approach separation by very small steps in x. However, the separation point x_s can be located accurately by extrapolation. Accepting Terrill's value of $x_s/a = 1.8230$, we observe the marked improvement in the results near separation and in the predicted separation point (obtained with the same step sizes) when the x-derivative terms are discretized by means of differences based on G^2 rather than on $1/G$.

Computations were also made for the circular cylinder with homogeneous suction. When the suction parameter S has the value $\sqrt{2}/2$, this is the case first considered by Bussman and Ulrich[1] and calculated accurately by Terrill.[21] The separation point was computed accurately by the present method and found to be $x_s/a = 2.0016$ in agreement with Terrill's result. When $S = 5$ this is the non-separating flow computed by Watson[24] by an asymptotic method. For this flow the present iterative process always fails as the rear stagnation point is approached closely. This experimental observation agrees with the demonstration given in Ref. 18, p. 340 that no solution in the form of equation (5) seems to exist at a rear stagnation point. Also computed accurately was the separating flow for a cylinder with an initial impermeable part, followed by homogeneous suction with $S = 1.0$ applied from $x/a = 1$. Separation is predicted to occur at $x_s/a = 2.079$. The results of all these computations for the cylinder are shown graphically in Figs. 9 and 10.

Howarth's linearly retarded flow $U = 1 - x$ was finally computed. This problem affords probably the most stringent test of any numerical method. Numerical details are given in Table 2 with results obtained by others. The extrapolated value of x_s was found to be 0.1197 compared with the accepted value 0.1198 (Leigh[9]). It was, however, necessary to use a very small value of δs to get close enough to separation to predict x_s to this accuracy. It is interesting that we get precisely Leigh's value if we apply h^2-extrapolation to the predicted values of x_s for $\delta s = 1/512$ (0.1194) and $\delta s = 1/1024$ (0.1197).

5. Concluding Remarks

The steady two-dimensional incompressible laminar boundary-layer problem has been posed as an integral equation in Crocco variables and a numerical method of solution of this problem has been developed. Several non-separating flows have been computed by the method, particularly flows with discontinuous suction distributions and periodic flows. Some problems involving separation have also been computed.

Viewed as a marching procedure for solving a parabolic partial differential equation, the method is implicit and was found experimentally to be stable for all the combinations of step-sizes tried. This result is made plausible by the local stability analysis given in the Appendix. The stability of an explicit-type scheme is also examined. The crucial device required to make the method work is the double-field type of iteration for solving the integral equation. An analysis of the convergence of this process is given in the Appendix.

The method is quite simple conceptually. It is easy to program and the storage requirements are relatively small. The method was programmed throughout by the author, originally in Autocode and run on the Cambridge University Atlas (Titan) computer and latterly in FORTRAN and run on the Glasgow University KDF9 computer and on the Univac 1108 computer at the National Engineering Laboratory. To give an indication of computing times, it was found that with a step-size $\delta s = 1/64$ across the boundary layer the time to compute and print at each of 22 x-stations the velocity profiles, the boundary-layer characteristics c_f, δ_1, δ_2 and δ_3 and to predict the separation point to about 0·5 per cent for the circular cylinder was about 30 seconds on the Univac, an average of about 1·4 seconds per station.

REFERENCES

No.	Author(s)	Title, etc.

1   K. Bussmann and A. Ulrich   Die laminare Reibungsschicht am Kreiszlinder mit Absaugung und Ausblasen.
Untersuch. Mitt. dtsch. Luftfahrtf. No. 2073 (1944).

2   C. B. Cohen and E. Reshotko   Similar solutions for the compressible laminar boundary layer with heat transfer and pressure gradient.
N.A.C.A. Report 1293 (1956).

3   L. Fox   *The numerical solution of two-point boundary problems in ordinary differential equations.*
Oxford University Press (1957).

4   G. E. Gadd   The numerical integration of the laminar compressible boundary-layer equations, with special reference to the problem of separation when the wall is cooled.
A.R.C. C.P. 312 (1952).

5   D. R. Hartree and J. R. Womersley   A method for the numerical or mechanical solution of certain types of partial differential equations.
Proc. Roy. Soc., A 161, 353 (1937).

6   P. Henrici   *Elements of numerical analysis.*
John Wiley & Sons (1964).

7   F. B. Hildebrand   *An introduction to numerical analysis.*
McGraw-Hill (1956).

8   E. Isaacson and H. B. Keller   *Analysis of numerical methods.*
John Wiley & Sons (1966).

9   D. C. F. Leigh   The laminar boundary-layer equation: a method of solution by means of a digital computer.
Proc. Camb. Phil. Soc., 51, 320 (1955).

10   R. D. Mills   The steady laminar incompressible boundary-layer problem as an integral equation in Crocco variables: investigation of the similarity flows.
A.R.C. R. & M. 3515 (1966).

11   R. D. Mills   Boundary-layer flow having periodically-distributed suction.
Z. angew. Math. Phys., 17, 577 (1966).

12   R. D. Mills   Numerical and experimental investigations of the shear layer between two parallel streams.
J. Fluid Mech., 33, 591 (1968).

13   R. D. Mills   Numerical solutions of viscous flow through a pipe orifice at low Reynolds numbers.
J. Mech. Eng. Sci., 10, 133 (1968).

14   R. D. Mills   On boundary-layer suction through narrow slots.
Quart. J. Mech. Appl. Math., 24, 461 (1971).

No.	Author(s)	Title, etc.

15 A. R. Mitchell .. .. .. *Computational methods in partial differential equations.*
John Wiley & Sons (1969).

16 G. M. Phillips .. .. .. Analysis of numerical iterative methods for solving integral and integrodifferential equations.
Comp. J., 13, 297 (1970).

17 W. Rheinboldt .. .. .. Zur Berechnung stationärer Grenzchichten bei kontinuierlicher Absaugung mit unstetig verländerlicher Absaugegeschwindikeit.
J. rat. Mech. Anal., 5, 539 (1956).

18 L. Rosenhead (Ed.) .. .. .. *Laminar boundary layers.*
Oxford University Press (1963).

19 W. Schönauer .. .. .. Ein Differenzenverfahren zur Lösing der Grenzschichtgleichung für stationäre, laminare, inkompressible Strömung.
Ingenieur-Archiv 33, 173 (1964).

20 A. M. O. Smith and D. W. Clutter Machine calculation of the incompressible laminar boundary-layer equations.
A.I.A.A. J. 1, 2062 (1963).

21 R. M. Terrill .. .. Laminar boundary-layer flow near separation with and without suction.
Phil. Trans. Roy. Soc. A 253, 55 (1960).

22 A. Thom .. .. The flow past circular cylinders at slow speeds.
Proc. Roy. Soc. A 141, 651 (1933).

23 R. Varga .. .. *Matrix iterative analysis.*
Prentice-Hall (1962).

24 E. J. Watson .. .. The asymptotic theory of boundary-layer flow with suction.
A.R.C. R. & M. 2619 (1947).

25 H. Weyl .. .. Concerning the differential equations of some boundary-layer problems.
Proc. nat. Acad. Sci. Wash., 27, 578 (1941).

26 J. H. Wilkinson .. .. .. *The algebraic eigenvalue problem.*
Oxford University Press (1965).

27 D. M. Young .. .. .. *Iterative solution of large linear systems of equations.*
Academic Press (1971).

APPENDIX

A1 Convergence of the Iterative Processes

A.1.1. Simplified problem. Insight into the difficulty of obtaining convergence in the full boundary-layer problem can best be gained by first considering a simplified problem. The essential character of the boundary-layer problem and the essential numerical difficulties are contained in the equation

$$G = \frac{P(x)}{G} + X\left(\frac{1}{G} - \frac{1}{G(x - \delta x)}\right) = \phi(G, X),$$ (A-1)

where $P(x)$ is analogous to the pressure-gradient parameter and X is $x/\delta x$. For typical boundary-layer-like situations this equation has two solutions, one negative and one positive, the latter being the desired physical solution. For instance, if $P(x) = \text{const.} = 1$ these two solutions are $G = -1$ and $G = 1$ for all X, the latter being the desired solution.

It is clear that any attempt to find the desired solution by simple iteration

$$G^{(n+1)} = \phi(G^{(n)}, X)$$ (A-2)

will be bedevilled by the presence of the (large) factor X, for if we define

$$r^{(n)} = P(x)/\{G^{(n)}\}^2 \quad \text{and} \quad t^{(n)} = 1/\{G^{(n)}\}^2$$ (A-3)

the condition for convergence is

$$\left|\frac{\partial \phi}{\partial G}(\bar{G}^{(n)})\right| = |\bar{\phi}'^{(n)}| = |\bar{r}^{(n)} + X\bar{t}^{(n)}| < 1, \quad G^{(n)} < \bar{G}^{(n)} < G,$$ (A-4)

for all iterates $G^{(n)}$ in a neighbourhood of the solution G. This condition is generally violated for all $X \geqslant 0$. For instance, with $P(x) = 1$ we find the condition is *asymptotically* $|1 + X| < 1$.

Suppose now we introduce a single relaxation factor ω so that the iterative process is

$$G^{(n+1)} = \omega\phi(G^{(n)}) + (1 - \omega)G^{(n)}.$$ (A-5)

The condition for convergence is now

$$K(\omega) = |\omega\bar{\phi}'^{(n)} + 1 - \omega| < 1.$$ (A-6)

As $\phi'^{(n)}$ is generally less than unity in most boundary-layer-like situations ω must lie in the range

$$0 < \omega < 2/(1 - \bar{\phi}'^{(n)})$$ (A-7)

(if $\phi'^{(n)} > 1$ it is necessary to use negative values of ω, *see* Isaacson and Keller, 8, p. 120). For optimum (Newton-like) convergence

$$\omega_{\text{opt}} = 1/(1 - \bar{\phi}'^{(n)}).$$ (A-8)

Using the solution value for G we find these conditions are asymptotically

$$0 < \omega < 2/(1 + r + Xt)$$ (A-9)

and

$$\omega_{\text{opt}} = 1/(1 + r + Xt).$$ (A-10)

The range of convergence is shown for $P = 1$ in Fig. 11.

13

The relaxation factor must clearly be decreased as X increases and the rate of convergence becomes increasingly sensitive to very slight changes in ω. Without a knowledge of the derivative $\phi'^{(n)}$ at each stage of the iteration it would be difficult to get good convergence. This difficulty is further complicated by the fact that ϕ' should be evaluated at some unknown value $\bar{G}^{(n)}$ between $G^{(n)}$ and G, though when $G^{(n)}$ is close to G then $\phi'^{(n)} \approx \bar{\phi}'^{(n)} \approx \phi'$.

In this simplified problem we could of course circumvent the difficulty of the large factor X by iterating with equation (A-1) in a different form. In the full integral-equation boundary-layer problem it is also possible to rearrange the equations to avoid this difficulty, but this would require the inversion of a 'full' matrix at each cycle of iteration. Thus if we are to succeed with our plan of using only simple iteration, it becomes necessary to face up to the problem of achieving convergence with the equations in the form of equation (A-1).

Suppose we re-write equation (A-1) as the two simultaneous equations

$$G = \frac{P(x)}{G} + F = \Phi(G, F)$$

and

(A-11)

$$F = X\left(\frac{1}{G} - \frac{1}{G(x - \delta x)}\right) = \chi(G).$$

Now consider the following iterative scheme with two relaxation factors ω and ω':

$$F^{(0)} = 0,$$

$$G^{(n+1)} = \omega\Phi(G^{(n)}, F^{(n)}) + (1 - \omega)G^{(n)}$$

(A-12)

and

$$F^{(n+1)} = \omega'\chi(G^{(n+1)}) + (1 - \omega')F^{(n)}.$$

Defining the 'errors' $\varepsilon^{(n)} = G^{(n)} - G$ and $\delta^{(n)} = F^{(n)} - F$, we find

$$\varepsilon^{(n+1)} = \left\{1 - \omega + \omega\frac{\partial\bar{\Phi}^{(n)}}{\partial G}\right\}\varepsilon^{(n)} + \omega\delta^{(n)} = a\varepsilon^{(n)} + b\delta^{(n)}$$

and

(A-13)

$$\delta^{(n+1)} = \left\{\omega'\frac{d\bar{\chi}^{(n+1)}}{dG}\right\}\varepsilon^{(n+1)} + (1 - \omega')\delta^{(n)} = c\varepsilon^{(n+1)} + d\delta^{(n)},$$

which is in a *Gauss–Seidel* or *Liebmann* form. It is not difficult to show that the matrix equation governing the propagation of errors is

$$\varepsilon^{(n+1)} = M^{(n)}\varepsilon^{(n)}$$

(A-14)

where the *iteration matrix* is given by

$$M^{(n)} = \begin{bmatrix} a & b \\ ca & cb + d \end{bmatrix}$$

(A-15)

and $\varepsilon = \{\varepsilon, \delta\}$ is the vector of errors.

For the iterative process (A-12) to converge the *spectral radius* of this matrix must be less than unity for all iterates in the neighbourhood of the solution (G, F). At solution, $M^{(n)}$ has the form

$$M = \begin{bmatrix} 1 - \omega(1 + r) & \omega \\ -\omega'Xt\{1 - \omega(1 + r)\} & 1 - \omega'(1 + \omega Xt) \end{bmatrix}.$$

(A-16)

14

The eigenvalues of this matrix are the same as those of the matrix

$$M' = \begin{bmatrix} 1 - \omega(1 + r) & -\omega\omega' Xt \\ 1 - \omega(1 + r) & 1 - \omega'(1 + \omega Xt) \end{bmatrix}$$

(A-17)

since the multiplication of the qth row of a matrix by a constant γ and the qth column by $1/\gamma$ leaves the eigenvalues unchanged. This form of the iteration matrix shows how the large factor X is offset by the quadratically small term $\omega\omega'$ when ω and ω' are both small.

The usual sufficient conditions for convergence (*viz.* row and column absolute sums <1) do not provide any information how to prescribe ω and ω' for convergence. In fact, these conditions are usually violated when ω and ω' have values which do give convergence. This is unfortunately true also of the full-scale problem.

In the present simplified problem we can, however, readily evaluate the eigenvalues of the matrix M' and determine that region of the (ω, ω')-plane which gives convergence. Figs. 12 and 13 show the region of convergence in the positive quarter-plane for two x-stations in a 'separating' type of flow. The latter was obtained by using the value of $P(x)$ for a circular cylinder, *viz.* $x \cot x$, in equation (A-1). Solution values for G were obtained by performing a step-by-step integration of the differential form of equation (A-1) by the Runge–Kutta method.

As X increases the outer curved boundary moves inwards towards the origin as shown in Fig. 12, and so it is necessary to reduce ω and ω' to maintain convergence. The points labelled N and N' with coordinates as shown in the figure correspond to conditions of optimum (Newton-like) convergence. The simple iterative scheme (A-5) with a single relaxation factor corresponds to the line $\omega' = 1$ in this figure. The 'narrow' region for convergence is clearly evident (compare Fig. 11). Thus we see that the rather sensitive requirement for convergence on a single factor ω has been replaced by a much less sensitive requirement on two factors ω and ω'.

The difficulties associated with separation can be appreciated by noting (*see* equation (A-3)), that as r passes below -1 and separation conditions begin to be approached, the region of convergence becomes squeezed in between two curves moving as shown in Fig. 13. As x increases beyond $2 \cdot 0$ to 'separation' (at $\approx 3 \cdot 0$) this region becomes very small indeed. Thus if we put $\omega' = \omega$ and maintain convergence by moving towards the origin along the line $\omega = \omega'$ we will soon 'miss' the convergence zone. However, we can still obtain convergence by using *positive* values of ω and ω' if we can find the appropriate region. This does not appear to be true of the full-scale problem.

A.1.2. Integral-equation problem. There is evidently some qualitative resemblance between the convergence of the iterative schemes equations (A-5) and (A-12) for the simplified problem and the corresponding schemes equations (20) and (21) for the full boundary-layer problem. In discussing the convergence of iterative methods for integral equations it is usual to try to determine a Lipschitz constant for the kernel and to examine whether this is less than unity (e.g. *see* Phillips[16]). This approach does not seem to lead to a natural extension of the analysis just presented for the simplified problem. Consequently, convergence was examined from the matrix point of view of the discretized problems ($i = 1, \ldots, N$)

$$G^{(n+1)}(s_i, x) = \omega\phi_i(\mathbf{G}^{(n)}(x)) + (1 - \omega)G^{(n)}(s_i, x)$$

(A-18)

and

$$F^{(0)}(s_i, x) = 0,$$

$$G^{(n+1)}(s_i, x) = \omega\Phi_i(\mathbf{G}^{(n)}(x), \mathbf{F}^{(n)}(x)) + (1 - \omega)G^{(n)}(s_i, x),$$

(A-19)

$$F^{(n+1)}(s_i, x) = \omega'\chi_i(\mathbf{G}^{(n+1)}(x)) + (1 - \omega')F^{(n)}(s_i, x),$$

where

$$\chi_i(\mathbf{G}^{(n+1)}(x)) = X\left(\frac{1}{G^{(n+1)}(s_i, x)} - \frac{1}{G(s_i, x - \delta x)}\right).$$

(A-20)

These are the scalar forms of the ith equations in equations (20) and (21) respectively, with $G^{(n)}(0, x) = 0$ from the boundary condition at the outer edge of the boundary layer. For simplicity of analysis the x-derivative terms are approximated by the usual two-point Lagrangian formula and the integrals by the Trapezium rule.

We are now discussing the convergence of the iterative solution of a set of non-linear algebraic equations (*see*, for example, Isaacson and Keller, 8, p. 109).

By an obvious generalisation of the analysis of the simplified problem (A.1.1) we find for simple iteration, using a single relaxation factor ω, that the matrix governing the growth of the vector of errors $\varepsilon(x) = \{\varepsilon_1, \varepsilon_2, \ldots, \varepsilon_N\}$, where

$$\varepsilon_i^{(n)}(x) = G^{(n)}(s_i, x) - G(s_i, x) = G_i^{(n)}(x) - G_i(x), \tag{A-21}$$

is

$$\varepsilon^{(n+1)} = M^{(n)}\varepsilon^{(n)} \tag{A-22}$$

where

$$M^{(n)} = I - \omega(I + R^{(n)} + XT^{(n)}), \tag{A-23}$$

$$R(\mathbf{s}, x) = \left(\frac{\alpha_{ij}}{G_j^2}\right) = \delta s \begin{bmatrix} \dfrac{\frac{1}{2}(l_1 + s_1^2 n_1)}{G_1^2} & \dfrac{s_1^2 n_2}{G_2^2} & \ldots\ 0 \\[2ex] \dfrac{l_1}{G_1^2} & \dfrac{\frac{1}{2}(l_2 + s_2^2 n_2)}{G_2^2} & \ldots\ 0 \\[2ex] \ldots & \ldots & \ldots\ 0 \\[2ex] \dfrac{l_1}{G_1^2} & \dfrac{l_2}{G_2^2} & \ldots\ \dfrac{\frac{1}{2}l_N}{G_N^2} \end{bmatrix}, \tag{A-24}$$

$$T(\mathbf{s}, x) = \left(\frac{\beta_{ij}}{G_j^2}\right) = \delta s \begin{bmatrix} \dfrac{\frac{1}{2}(m_1 + s_1^2 q_1)}{G_1^2} & \dfrac{s_1^2 q_2}{G_2^2} & \ldots 0 \\[2ex] \dfrac{m_1}{G_1^2} & \dfrac{\frac{1}{2}(m_2 + s_2^2 q_2)}{G_2^2} & \ldots 0 \\[2ex] \ldots & \ldots & \ldots 0 \\[2ex] \dfrac{m_1}{G_1^2} & \dfrac{m_2}{G_2^2} & \ldots 0 \end{bmatrix}, \tag{A-25}$$

$$l_i(x) = 2(1 + 5P)s_i^3 - 2(1 + 3P)s_i^5, \qquad m_i = 4(s_i^3 - s_i^5),$$

$$n_i(x) = 2(1 + P)(s_i - s_i^3), \qquad q_i = 4(s_i - s_i^3), \tag{A-26}$$

$$G_i(x) = G(s_i, x), \quad s_i = i\delta s \quad \text{for } i = 1, \ldots, N$$

and I is the $N \times N$ unit matrix.

For convergence the spectral radius of the matrix $M^{(n)}$ must be less than unity for all iterates in a neighbourhood of the solution, though for convenience we will omit the iteration index n in most of the following. Let the eigenvalues of the matrix $R + XT$ be denoted by v and those of M by λ; then they are connected by the linear transformation

$$\lambda = 1 - \omega(1 + v) \tag{A-27}$$

in the complex plane (Isaacson and Keller, 8, p. 73). The unit circle in the λ-plane maps into the circle C, centre $((1 - \omega)/\omega, 0)$ and radius $1/\omega$, in the v-plane. Hence for convergence the parameter ω must be chosen so that the circle C covers all the eigenvalues v_k of $R + XT$. This circle always passes through the point $(-1, 0)$ and so

with positive values of ω it is always *necessary* that

$$Re(v) > -1 \qquad\qquad (A\text{-}28)$$

for convergence (for negative ω, $Re(v) < 1-$). A sufficient condition for convergence is that C covers the *union* of all the row *Gerschgorin discs* of $R + XT$. (*see* Wilkinson[26] for the definition of the Gerschgorin discs of a matrix).

Now it is clear from the last row of the matrix $R + XT$ and equations (A-24) to (A-26) that there exists a row Gerschgorin disc of radius $\sum_{j=1}^{N-1} \delta s |l_j| + X m_j|/G_j^2$ centred at the point $(2\,\delta s P(x)/G_N^2, 0)$. Since X increases rapidly on marching in the x-direction, this disc will quickly expand and pass through the left of the circle C, no matter how much ω is reduced and no matter the nature of $P(x)$. Hence (A-28) will soon become violated and the single-relaxation-factor process will fail after only a few steps in the x-direction, as was observed experimentally.

We can now give an explanation of the difficulties encountered on approaching 'separation' conditions in the computation of the similarity flows (*see* Ref. 10). For these flows only the R matrix is involved and we will set $v = \mu$ in this special case. First, assume all the eigenvalues of R are real and arranged in descending order $\mu_1 > \mu_2 > \ldots > \mu_N$. The conditions for convergence are

$$0 < \omega < 2/(1 + \mu_1) \qquad\qquad (A\text{-}29)$$

and

$$\mu_N > -1, \qquad\qquad (A\text{-}30)$$

with optimum convergence when

$$\omega = \omega_{\text{opt}} = \frac{1}{1 + \frac{1}{2}(\mu_1 + \mu_N)} \qquad\qquad (A\text{-}31)$$

given by

$$\lambda_{\text{min}} = \frac{\mu_1 - \mu_N}{2 + \mu_1 + \mu_N}. \qquad\qquad (A\text{-}32)$$

Hence the range of ω for convergence depends on the magnitude of the largest positive eigenvalue μ_1, while the rate of convergence diminishes to zero as the smallest eigenvalue $\mu_N \to -1$ from above, whatever the value of μ_1.

It is clear from (A-24) and (A-26) that

$$\mu_m = 2P\delta s/G_N^2 \qquad\qquad (A\text{-}33)$$

is *an* eigenvalue of R, though not necessarily the smallest. Near 'separation' conditions P becomes negative and the wall shear stress term G_N tends to zero. Hence μ_m will soon approach and pass below -1 and so the number of iterations to convergence will increase but ultimately the process will fail no matter how small ω is made. This was precisely what was found by numerical experiment in I. In general all the eigenvalues of R may not be real and we cannot make simple statements like (A-31) and (A-32) about optimum convergence. However, μ_m is always an eigenvalue of R and the necessary condition (A-28) or (A-30) will eventually become violated by μ_m when separation conditions are approached closely.

It also becomes clear why large positive values of the suction parameter W lead to strengthened convergence.[10] Though W does not enter explicitly into the convergence analysis, it enters implicitly by giving increased values of the wall shear stress term G_N (and the other G_i generally). Hence in particular μ_m will diminish in absolute value, as will the other μ_k, as W is increased. Thus the covering circle C can be reduced in size, that is, ω can be increased for convergence. The converse effect will occur for large blowing rates.

By a straightforward generalisation of the two-relaxation-factor convergence analysis for the simplified problem, we find the equation governing the propagation of the $2N \times 1$ vector of errors $\mathbf{e} = \{\varepsilon, \delta\}$, where

$$\varepsilon_i^{(n)} = G_i^{(n)} - G_i, \quad \delta_i^{(n)} = F_i^{(n)} - F_i,$$

17

is now

$$\mathbf{e}^{(n+1)} = M_2^{(n)}\mathbf{e}^{(n)}, \tag{A-34}$$

where M_2 is now the $2N \times 2N$ partitioned matrix

$$M_2 = \begin{bmatrix} A & B \\ CA & CB + D \end{bmatrix}, \tag{A-35}$$

A, B, C and D are the $N \times N$ matrices

$$\begin{aligned} A &= I - \omega(I + R), & B &= \omega Q, \\ C &= -\omega'X \operatorname{diag}(1/G_1^2, \ldots, 1/G_N^2), & D &= (1 - \omega')I, \end{aligned} \tag{A-36}$$

with R as defined in (A-24) and $Q = (\beta_{ij})$ (see (A-25)).

Now a similarity transform of the form SMS^{-1} where S is a non-singular matrix leaves the eigenvalues of M unchanged (see, for example, Wilkinson, 26, p. 6). Choosing

$$S = \begin{bmatrix} I & O \\ O & C^{-1} \end{bmatrix}, \quad \text{i.e. } S^{-1} = \begin{bmatrix} I & O \\ O & C \end{bmatrix}, \tag{A-37}$$

we find that under this transformation the matrix M_2 becomes

$$M_2' = \begin{bmatrix} A & BC \\ A & BC + D \end{bmatrix} = \begin{bmatrix} I - \omega(I + R) & -\omega\omega'XT \\ I - \omega(I + R) & I - \omega'(I + \omega XT) \end{bmatrix}. \tag{A-38}$$

The point of this transformation (as in the simplified problem) is to show how the factors ω and ω' come together and offset the growth of the factor X.

It is usual in discussing the convergence of linear systems to try to establish a relation between the eigenvalues of the iteration matrix $M_2'(\omega, \omega')$ and those of a related simpler matrix which is independent of the relaxation factors. This is the underlying idea of the classical S.O.R. methods. Such relations can usually be found only for very restricted classes of matrices (see Young,[27] p. 140). In the present case, the author has not been able to establish any such connection on account of the very general nature of the matrices R and T. The most that can be deduced in this direction seems to be the following particular relations:

$$\begin{aligned} \lambda &= 1 - \omega(1 + v) & \omega' &= 1, \\ (1 - \omega' - \lambda)^N(1 - \lambda)^N &= 0 & \omega &= 0, \end{aligned} \tag{A-39}$$

and

$$\left| R - \left(\frac{1 - \omega - \lambda}{\omega} \right)I \right|(1 - \lambda)^N = 0 \qquad \omega' = 0,$$

where the λ are the non-zero eigenvalues of M_2' and the v are the eigenvalues of $R + XT$. The first of these results tells us nothing we do not already know from the single-relaxation-factor process; the last two tell simply that convergence will not occur when either ω or ω' is zero, $\lambda = 1$ then being a root of multiplicity N. As the iterative process does in fact converge for small positive values of ω and ω', the matrix M_2' must be a *convergent matrix* for some region of the positive (ω, ω')-quarter-plane. It may be that there is some qualitative resemblance between this region and the region shown in Figs. 12 and 13 for the simplified problem.

We can, however, easily deduce a relation which determines how closely the separation point can be approached before our iterative process fails to converge. By expanding the determinant $|M_2' - \lambda I_2|$ along the $2N$th column and then the determinant so obtained along its Nth column, we easily see that

$$\lambda_{\omega'} = 1 - \omega', \tag{A-40}$$

$$\lambda_m = 1 - \omega(1 + v_m) = 1 - \omega \left\{ 1 + 2P(x)\frac{\delta s}{G_N^2} \right\} \tag{A-41}$$

18

are always eigenvalues of M'_2. Clearly, ω' must always be positive and <2 from (A-40). Also, by (A-41) the necessary condition (A-28) puts the restriction

$$P(x_l) > -\tfrac{1}{2}G_N^2/\delta s \qquad (A-42)$$

on the distance x_l one can approach the separation point when using positive values of ω. For a given flow, the smaller δs is made the nearer one can get to separation and this indeed was found to be the case experimentally. As noted earlier, the Aitken process enables one to get even closer. It is sometimes possible after (A-42) becomes violated to get a little nearer still by reversing the sign of the relaxation factor for G_N (i.e. putting $\omega_N = -\omega_N$ in (A-43) below) for then $|\lambda_m|$ becomes less than unity. This does not constrain all the other eigenvalues of M'_2 to lie inside the unit circle however, and so the device is likely to be of limited usefulness.

We have considered throughout only two scalar relaxation factors ω and ω'. The analysis generalises readily to case when they are replaced by the matrices

$$\Omega = \mathrm{diag}\,(\omega_1,\ldots,\omega_N) \quad \text{and} \quad \Omega' = \mathrm{diag}\,(\omega'_1,\ldots,\omega'_N), \qquad (A-43)$$

though we lack *a fortiori* some means of prescribing the ω_i and ω'_i for convergence.

For the circle flow, the matrices R and T and the various derived matrices were computed using solution values for $G(s_i, x)$ on a coarse mesh across the boundary layer. With the aid of a subroutine to compute the spectral radius of a general matrix it was verified that the simple iteration scheme (A-18) fails after a few steps in the x-direction. Furthermore, it was verified at several x-stations that the matrix $M'_2(\omega, \omega')$ was convergent for those values of ω and ω' which had given convergence in the two-field scheme (A-19).

A2. Stability

A.2.1. An explicit-type scheme. Suppose we replace the $\partial(1/G)/\partial x$ terms by the following difference formula involving function values at two previous x-stations,

$$\frac{\partial(1/G)}{\partial x}(s_i, x_j) = \frac{1}{\delta x}\left(\frac{1}{G(s_i, x_j - \delta x)} - \frac{1}{G(s_i, x_j - 2\delta x)}\right) = \frac{1}{\delta x}\left(\frac{1}{G_{i,j-1}} - \frac{1}{G_{i,j-2}}\right). \qquad (A-44)$$

This means when we iterate equation (10) the terms involving the factor $X = x/\delta x$ are not included in the iteration. This would seem to be a very convenient way of avoiding the difficulties of the large factor X inside the iteration. However, it was found experimentally that this process was *unstable* for all the $(\delta x, \delta s)$-pairs that were tried. We shall see why this is the case from the following *local matrix stability analysis*.

As the equations are non-linear we first have to linearise them by setting $G = G + g$ where $g(s, x)$ is a small perturbation. We shall again simplify the problem by using the Trapezium rule for the integrals. The set of linear equations which have to be solved to advance the perturbation solution g from the $(j-2)$th and $(j-1)$th x-stations to the jth x-station may be written in matrix form as,

$$\mathbf{g}_j = -X(I + R_j)^{-1}T_{j-1}\mathbf{g}_{j-1} + X(I + R_j)^{-1}T_{j-2}\mathbf{g}_{j-2}, \qquad (A-45)$$

where the matrices R and T are again given by (A-24) and (A-25). This is a *three-level* formula which can be reduced to a *two-level* formula by setting

$$\begin{bmatrix} \mathbf{g}_j \\ \mathbf{h}_j \end{bmatrix} = H \begin{bmatrix} \mathbf{g}_{j-1} \\ \mathbf{h}_{j-1} \end{bmatrix}, \qquad (A-46)$$

where

$$H = \begin{bmatrix} -X(I + R_j)^{-1}T_{j-1} & X(I + R_j)^{-1}T_{j-2} \\ I & O \end{bmatrix} \qquad (A-47)$$

is the $2N \times 2N$ *amplification matrix* (for example, *see* Mitchell, 15, p. 87). The eigenvalues of H are given by the roots of the determinantal equation

$$|\lambda^2(I + R_j) - \lambda X T_{j-1} - X T_{j-2}| = 0. \qquad (A-48)$$

19

Stability depends on the spectral radius of H being less than unity. It is clear that for fixed δx and δs this spectral radius must increase as x increases. In fact, it will soon become greater than unity and render the scheme useless. It is interesting to note that for a fixed value of the step-size δs, the tendency to instability becomes greater the smaller the step-size δx in the marching direction—which is the opposite tendency of the standard explicit methods for parabolic equations. It may be that the scheme is stable at any x-station for large enough δx and/or small enough δs—i.e. *conditionally stable*. The appropriate *stability criterion* is not readily deducible however, from the above analysis. The author is of the opinion that even if it exists it would make rather too stringent demands on the values of δx and δs for the scheme to be practicable. In any case, difference formulae of the type (A-44) are not very accurate.

A.2.2. Implicit scheme. We first replace the $\partial(1/G)/\partial x$-terms by the usual two-point formula:

$$\frac{\partial(1/G)}{\partial x}(s_i, x_j) = \frac{1}{\delta x}\left(\frac{1}{G(s_i, x_j)} - \frac{1}{G(s_i, x_j - \delta x)}\right) = \frac{1}{\delta x}\left(\frac{1}{G_{i,j}} - \frac{1}{G_{i,j-1}}\right). \tag{A-49}$$

On linearising and using the Trapezium rule for the integrals we find the equations that have to be solved to advance the perturbation solution from the $(j - 1)$th x-station to the jth x-station are

$$\mathbf{g}_j = H\mathbf{g}_{j-1}, \tag{A-50}$$

where the amplification matrix is now the $N \times N$ matrix

$$H = (I + R_j + XT_j)^{-1}XT_{j-1} \tag{A-51}$$

which is clearly of implicit type. One feels intuitively that the spectral radius of H should be less than unity for all X and δs when $R_j + XT_j$ and XT_{j-1} are *non-negative* matrices—which they are in all the cases considered in this report. Unfortunately, these matrices seem to be of too general a character for the well-known Perron–Frobenius theory to provide a proof that H is a convergent matrix (*see* Varga, 23, p. 30).

When we use the three-point formula for the x-derivative terms, the amplification matrix becomes

$$H = \begin{bmatrix} 2(I + R_j + \frac{3}{2}XT_j)^{-1}XT_{j-1} & -\frac{1}{2}(I + R_j + \frac{3}{2}XT_j)^{-1}XT_{j-2} \\ I & O \end{bmatrix}. \tag{A-52}$$

The crucial implicit nature of the scheme remains in evidence, however. Experimentally, the author found the scheme to be stable for every flow considered and every combination of step sizes.

The discussion of convergence and stability is a little more complicated when we use Simpson's rule and equations (17) and (18) for the x-derivative terms (i.e. differences on G^2). However, the general convergence and stability characteristics of the algorithm remain as described above. The author has verified directly the stability characteristics of schemes A.2.1 and A.2.2 for the circle flow by computing the spectral radii of the appropriate amplification matrices at solution using a coarse mesh across the boundary layer.

TABLE 1

x/a	$\dfrac{\tau_w}{\rho U^2}\left(\dfrac{U_\infty a}{\nu}\right)^{\frac{1}{2}}$			$\dfrac{\delta_1}{a}\left(\dfrac{U_\infty a}{\nu}\right)^{\frac{1}{2}}$			$\dfrac{\delta_2}{a}\left(\dfrac{U_\infty a}{\nu}\right)^{\frac{1}{2}}$		
	I	II	Terrill	I	II	Terrill	I	II	Terrill
0·04	0·13936	0·13936	0·1394	0·45289	0·45289	0·4583	0·20678	0·20678	0·2068
0·16	0·55222	0·55222	0·5221	0·46044	0·46045	0·4605	0·20768	0·20768	0·2077
0·80	2·1355	2·1355	2·1355	0·52379	0·52376	0·5238	0·23356	0·23355	0·2336
1·00	2·2569	2·2570	2·2568	0·5698	0·5697	0·5697	0·2517	0·2517	0·2517
1·60	1·2422	1·2441	1·2434	0·9368	0·9360	0·9363	0·3735	0·3733	0·3734
1·76	0·5480	0·5569	0·5538	1·2654	1·2600	1·2624	0·4452	0·4446	0·4451
1·80	0·2833	0·3054	0·2967	1·4461	1·4299	1·4373	0·4690	0·4680	0·4687
1·81	0·1998	0·2203	—	1·515	1·497	—	0·4754	0·4744	—
1·815	0·1464	0·1691	—	1·562	1·541	—	0·4787	0·4777	—
1·819	0·0881	0·1188	0·1066	1·617	1·586	1·5985	0·4814	0·4803	0·4812
1·820	0·0632	0·1032	—	1·642	1·600	—	0·4821	0·4810	—
1·821	*	0·0849	0·0724	—	1·618	1·631	—	0·4817	0·4825

Boundary-layer characteristics as functions of x for flow with external velocity $U = 2U_\infty \sin(x/a)$. The present computations were made with $\delta s = 1/512$, $\delta(x/a) = 0.04$ to $x/a = 1.80$, $\delta(x/a) = 0.0025$ to $x/a = 1.815$, $\delta(x/a) = 0.001$ to $x/a = 1.820$ and $\delta(x/a) = 0.0005$ thereafter. I and II denote results using finite differences in x-direction on $(1/G)$ and G^2 respectively. In case I extrapolated value of x_s is 1·8210, in case II 1·8230, compared with Terrill's value 1·8230. * denotes extrapolated to zero.

TABLE 2

x	$c_f\left(\dfrac{Ux}{2\nu}\right)^{\frac{1}{2}}$				$\delta_1\left(\dfrac{U}{2\nu x}\right)^{\frac{1}{2}}$	$\delta_2\left(\dfrac{U}{2\nu x}\right)^{\frac{1}{2}}$	$\delta_3\left(\dfrac{U}{2\nu x}\right)^{\frac{1}{2}}$
	Present	Smith, Clutter	Leigh	Hartree	Present	Present	Present
0·000	0·469600	0·469600	—	—	1·21678	0·46960	0·73848
0·025	0·41162	—	—	—	1·2878	0·48417	0·75833
0·050	0·34518	0·34496	—	0·34515	1·3776	0·50042	0·78003
0·075	0·26629	—	—	—	1·4988	0·5187	0·8038
0·100	0·1645	—	—	0·1652	1·6872	0·5396	0·8301
0·110	0·1091	0·1100	—	0·1093	1·8114	0·5489	0·8414
0·115	0·0725	0·0737	—	0·0718	1·906	0·5537	0·8472
0·117	0·0535	—	—	—	1·959	0·5557	0·8496
0·1175	0·0480	—	0·0494	—	1·976	0·5562	0·8502
0·118	0·0419	—	—	—	1·994	0·5567	0·8508
0·1185	0·0350	0·0373	—	0·0352	2·016	0·5572	0·8514
0·11875	0·0310	—	0·0317	—	2·028	0·5575	0·8517
0·11900	0·0265	—	—	—	2·043	0·5577	0·8520
0·11925	0·0207	—	0·0223	—	2·063	0·5580	0·8523
0·11950	0·0133	0·0202	0·0163	0·0161	2·10	0·5583	0·8526

Boundary-layer characteristics as functions of x for flow with external velocity $U = 1 - x$. The present computations were made with $\delta s = 1/1024$, $\delta x = 0.005$ to 0·110, $\delta x = 0.001$ to 0·116, $\delta x = 0.0005$ to 0·118, $\delta x = 0.00025$ thereafter. Extrapolated $x_s = 0.1197$, compared with Leigh's value 0·1198.
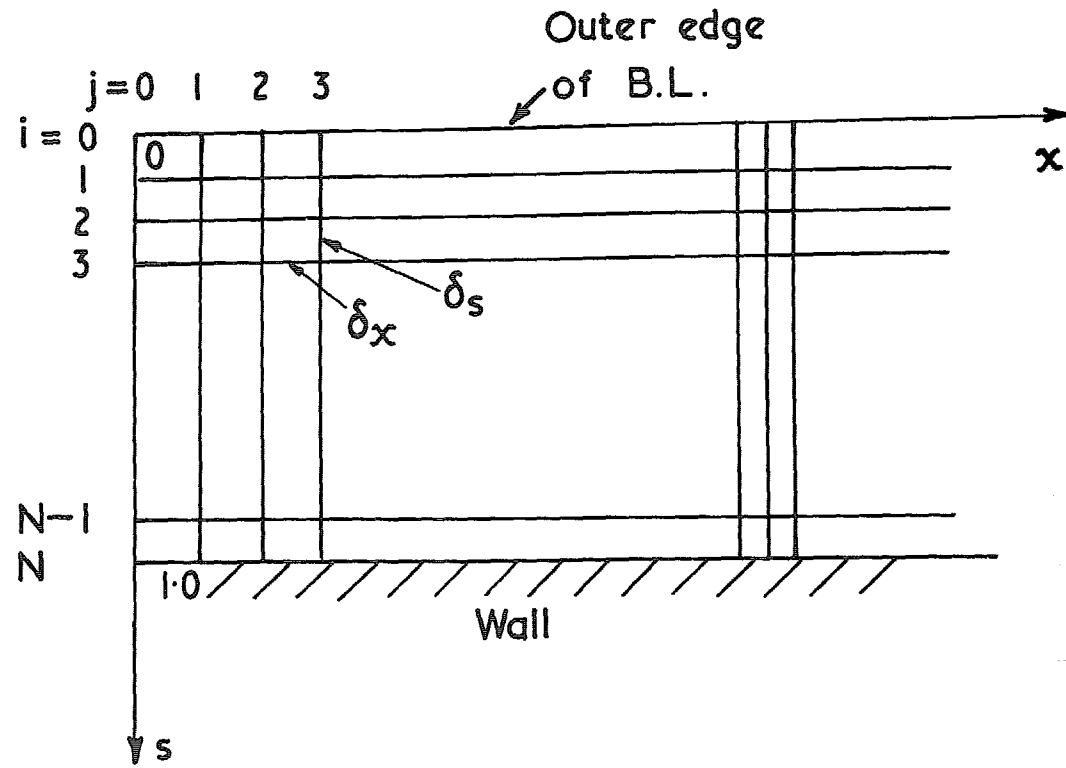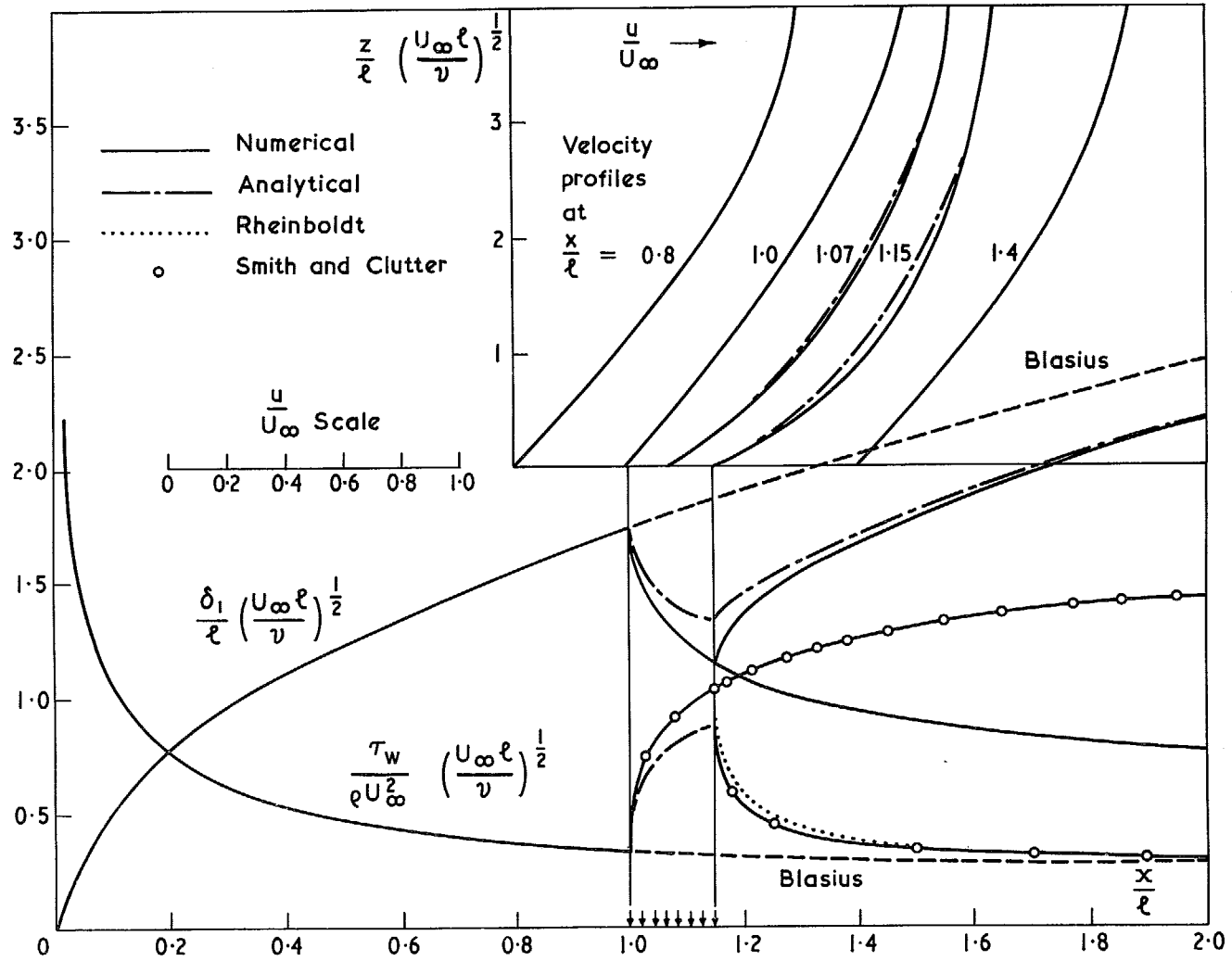
Fig. 1.

FIG. 2. Suction step and pulse. Velocity profiles, shear stress distributions and displacement thicknesses for $S = -(w_0/U_\infty)(U_\infty l/v)^{\frac{1}{2}} = 1.5$.
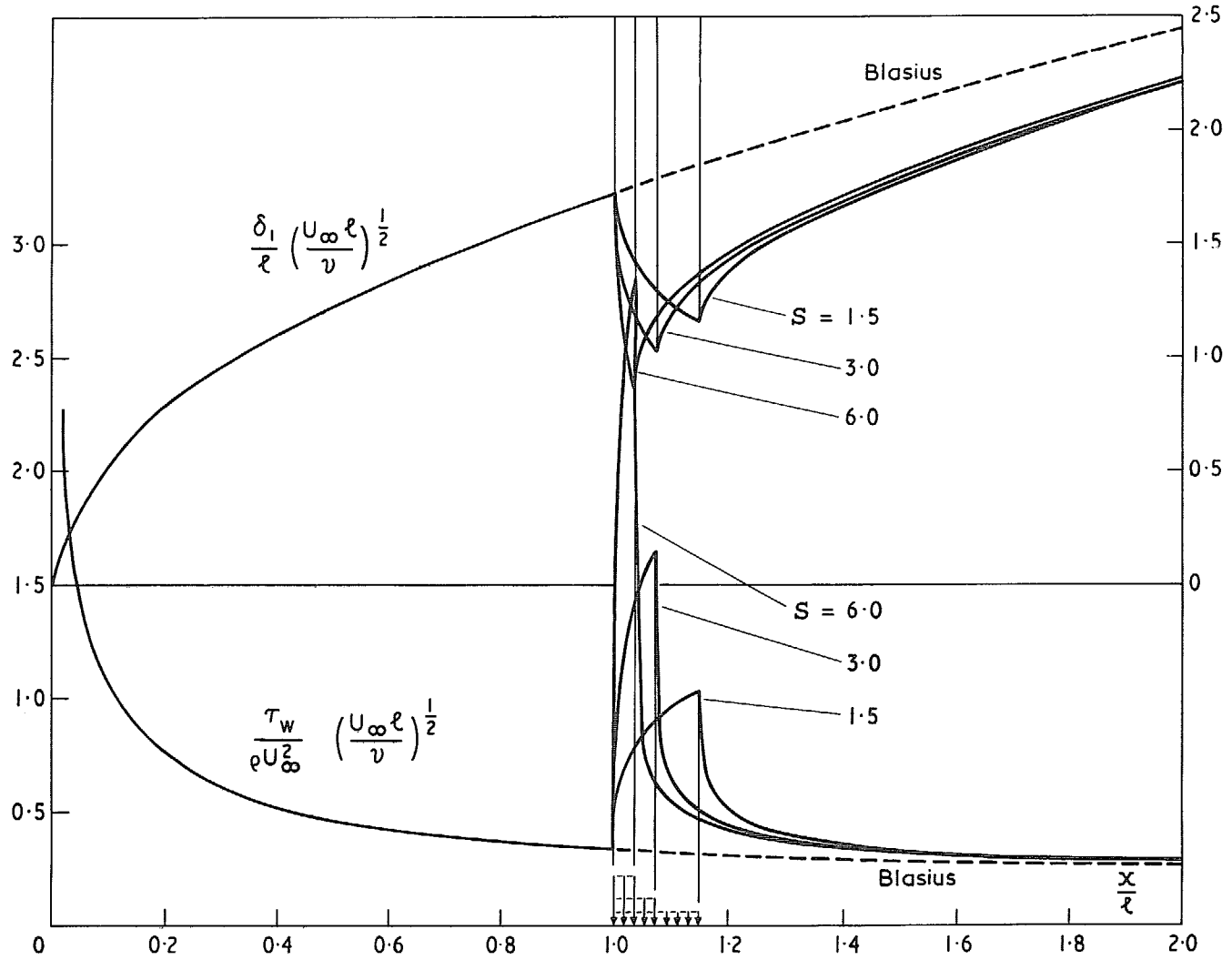
$$\frac{\delta_1}{\ell}\left(\frac{U_\infty \ell}{v}\right)^{\frac{1}{2}}$$

Blasius

S = 1·5

3·0

6·0

S = 6·0

3·0

1·5

$$\frac{\tau_w}{\rho U_\infty^2}\left(\frac{U_\infty \ell}{v}\right)^{\frac{1}{2}}$$

Blasius

$$\frac{x}{\ell}$$

FIG. 3. Suction pulse of varying width with same total suction quantity.
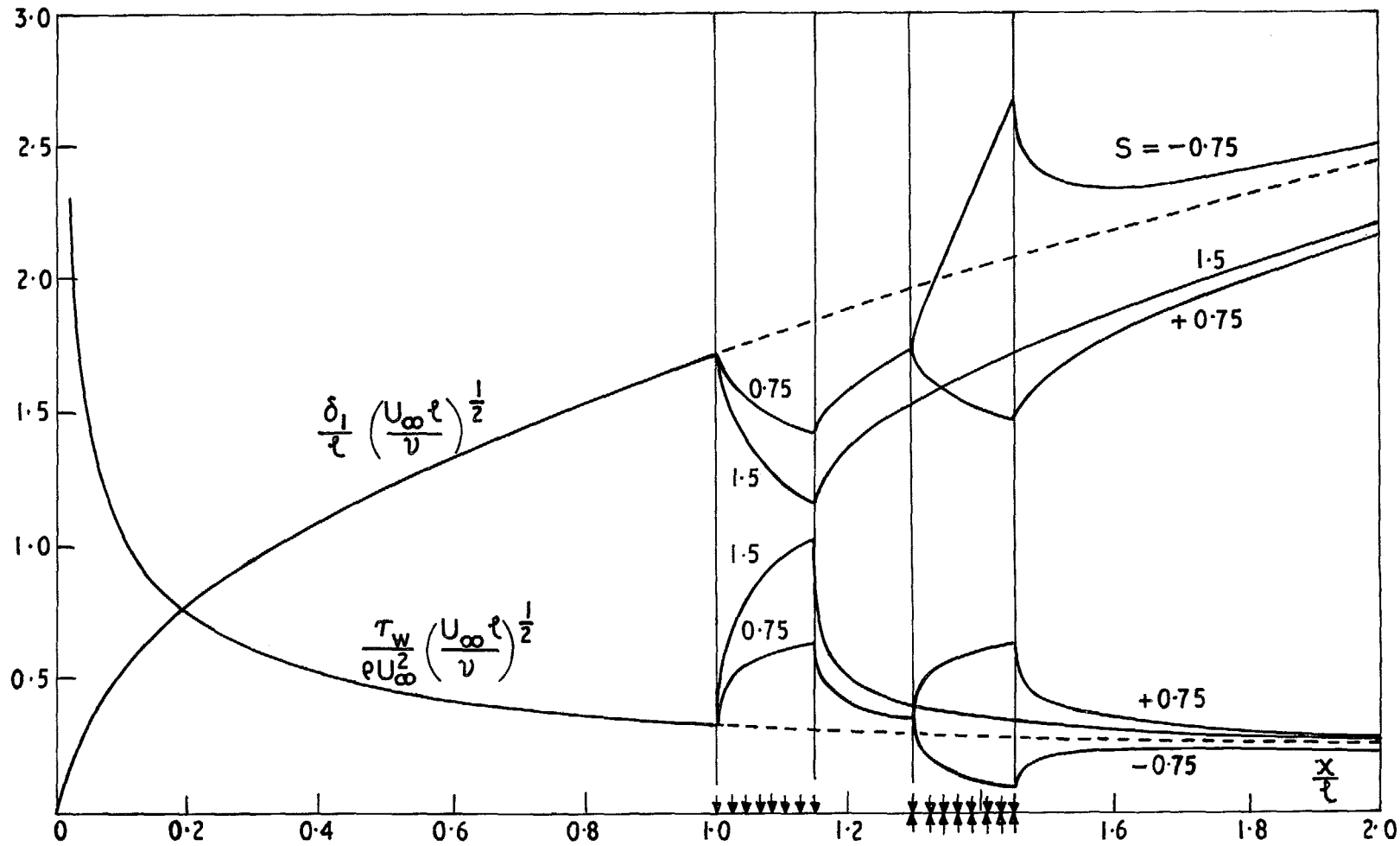
FIG. 4. Spaced suction and blowing pulses.

25
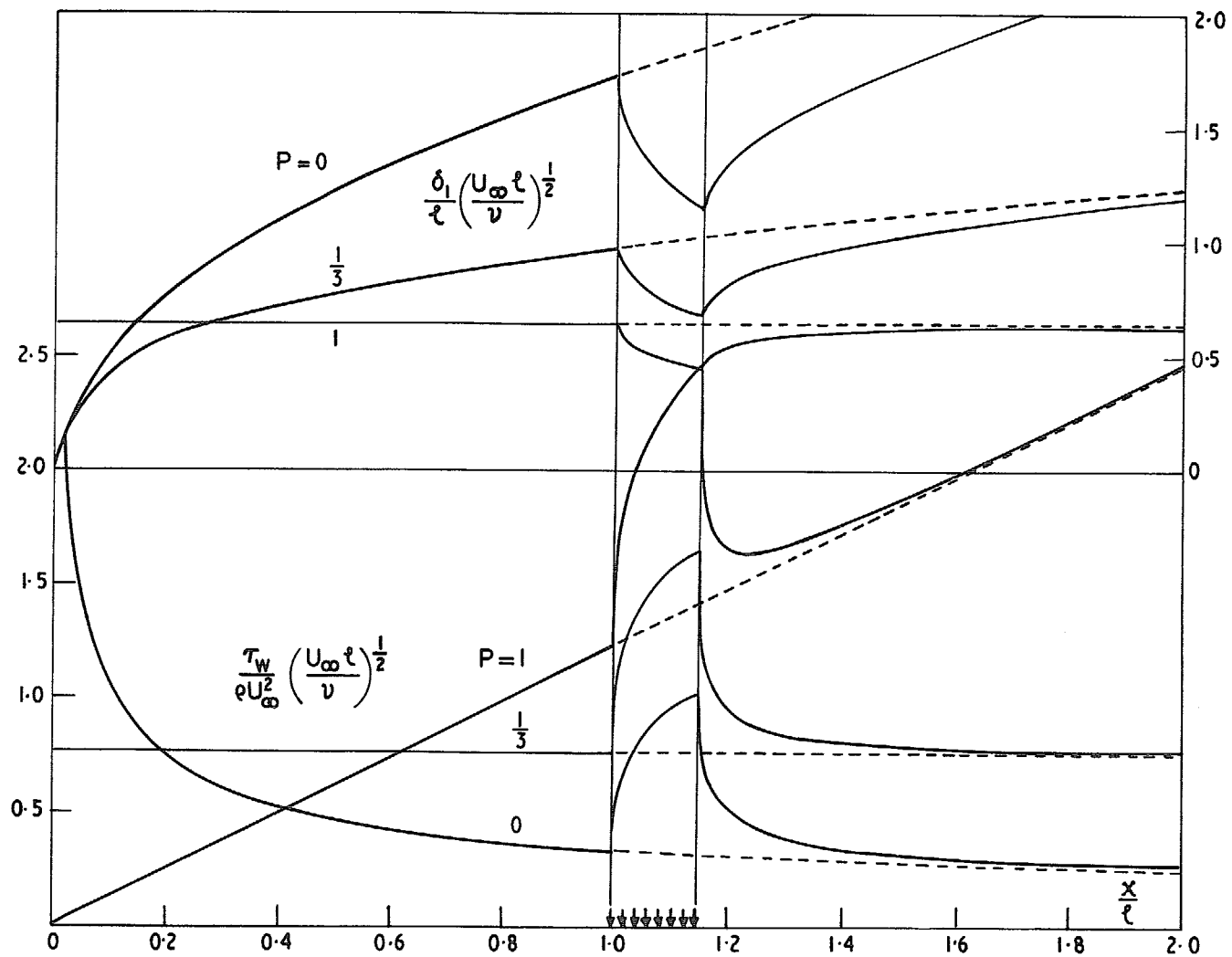
FIG. 5. Suction pulses in flat plate ($P = 0$), 90° wedge ($P = \frac{1}{3}$) and stagnation flow ($P = 1$).
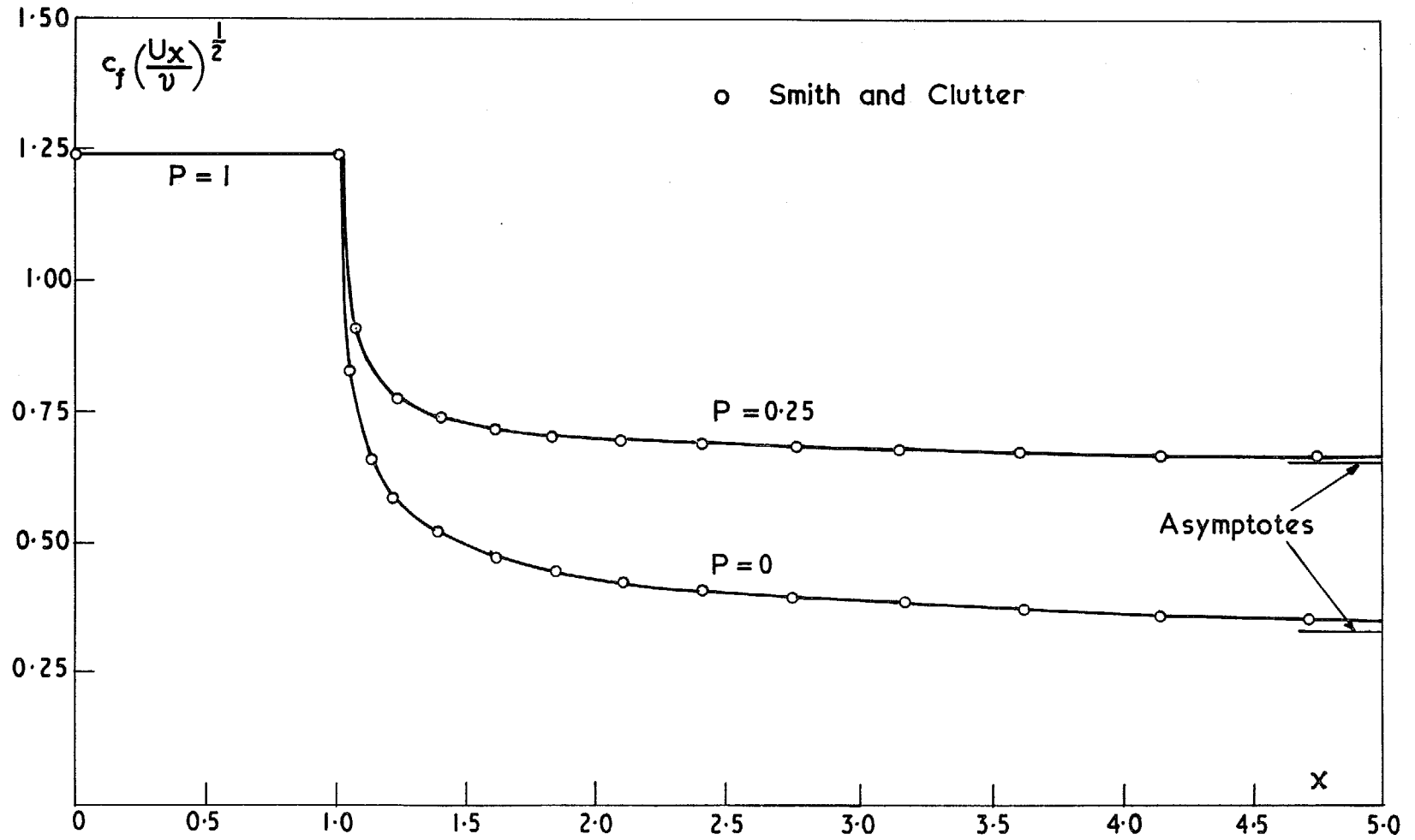
FIG. 6.   Step change in pressure gradient. Shear stress distribution.
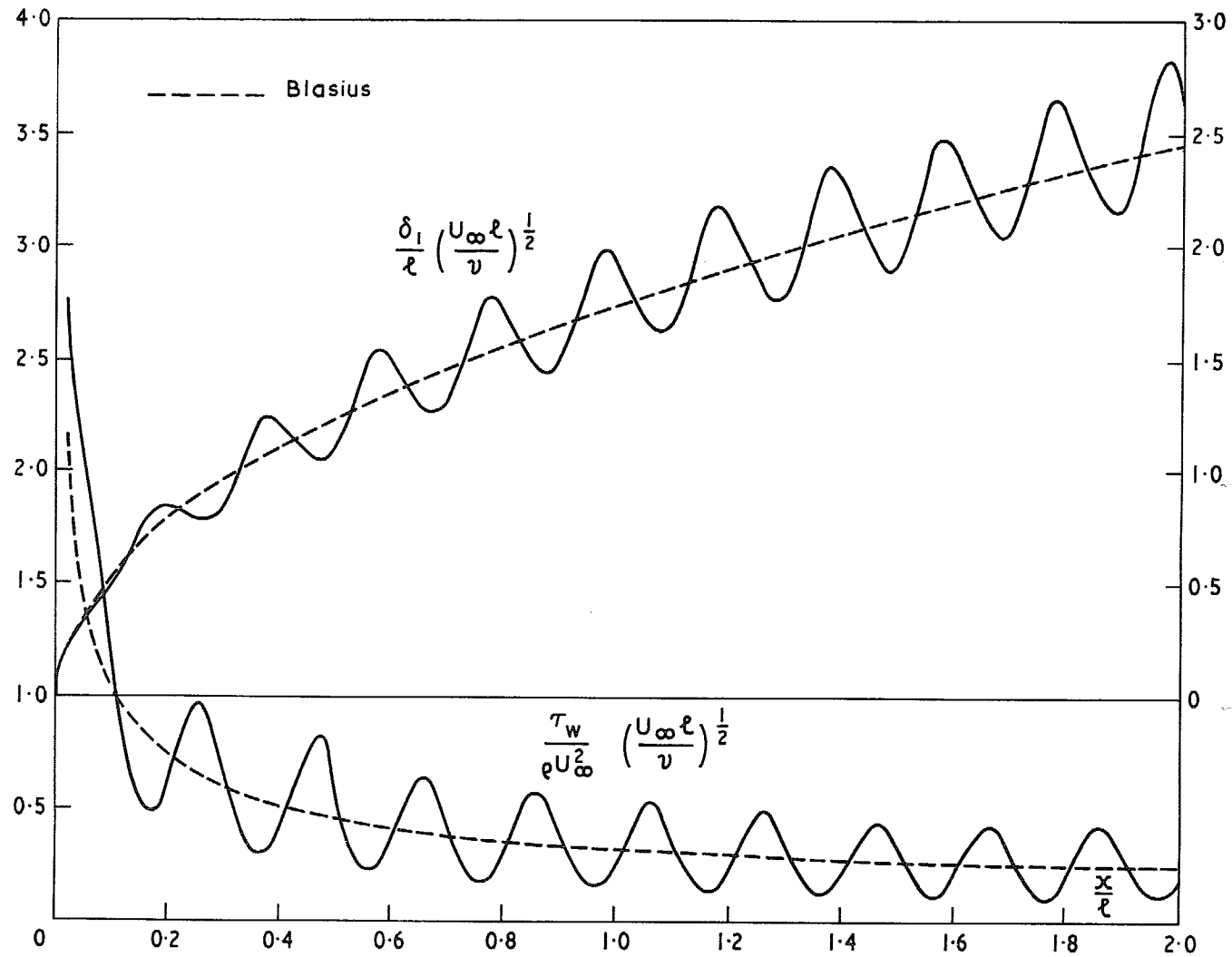
FIG. 7.   Periodic suction at wall $S(x) = S \sin (10\pi x/l)$ for $S = 1\cdot0$.
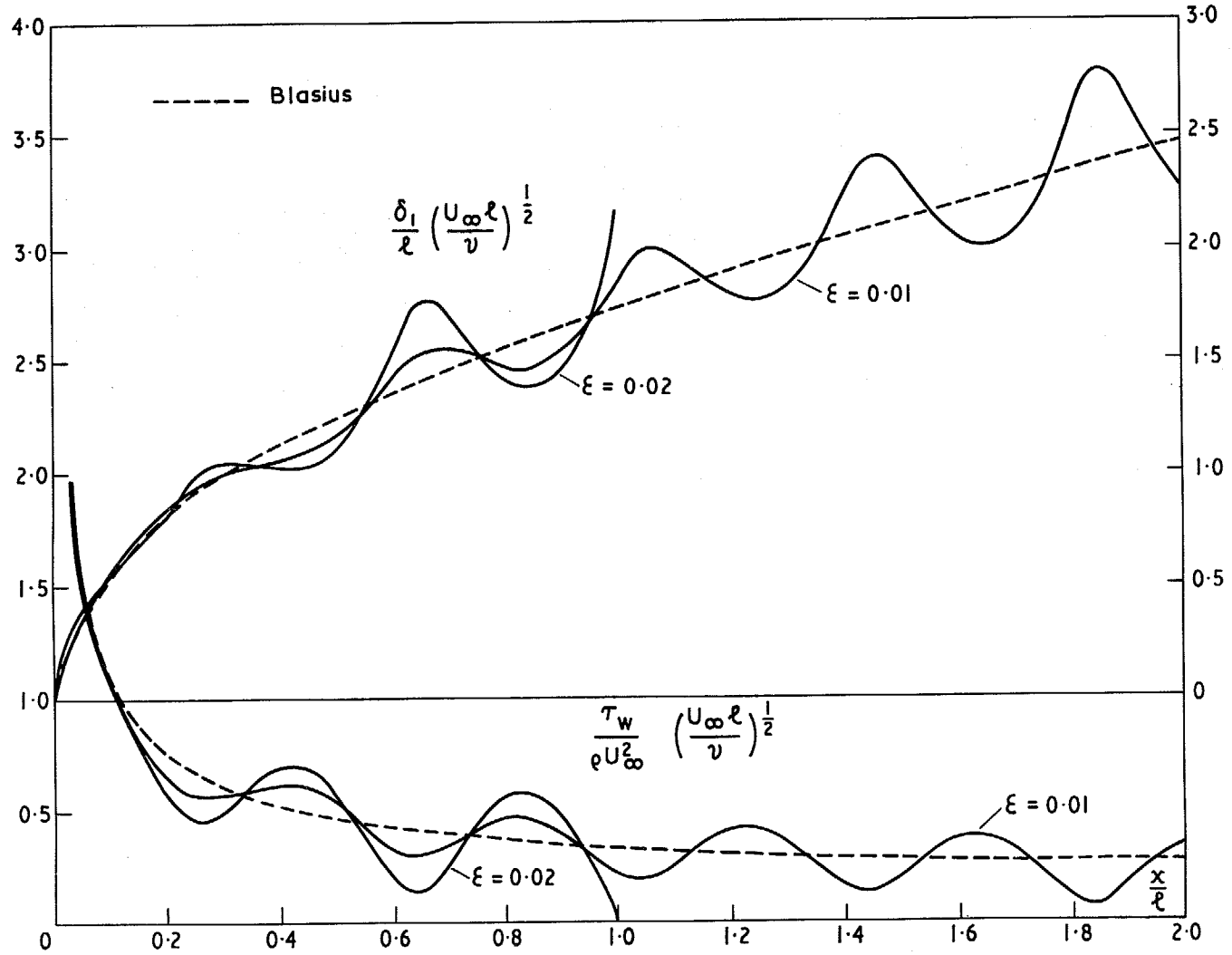
FIG. 8.   Periodic mainstream $u = u_\infty(1 + \varepsilon \sin (5\pi x/l))$ for $\varepsilon = 0.01$ and 0.02.
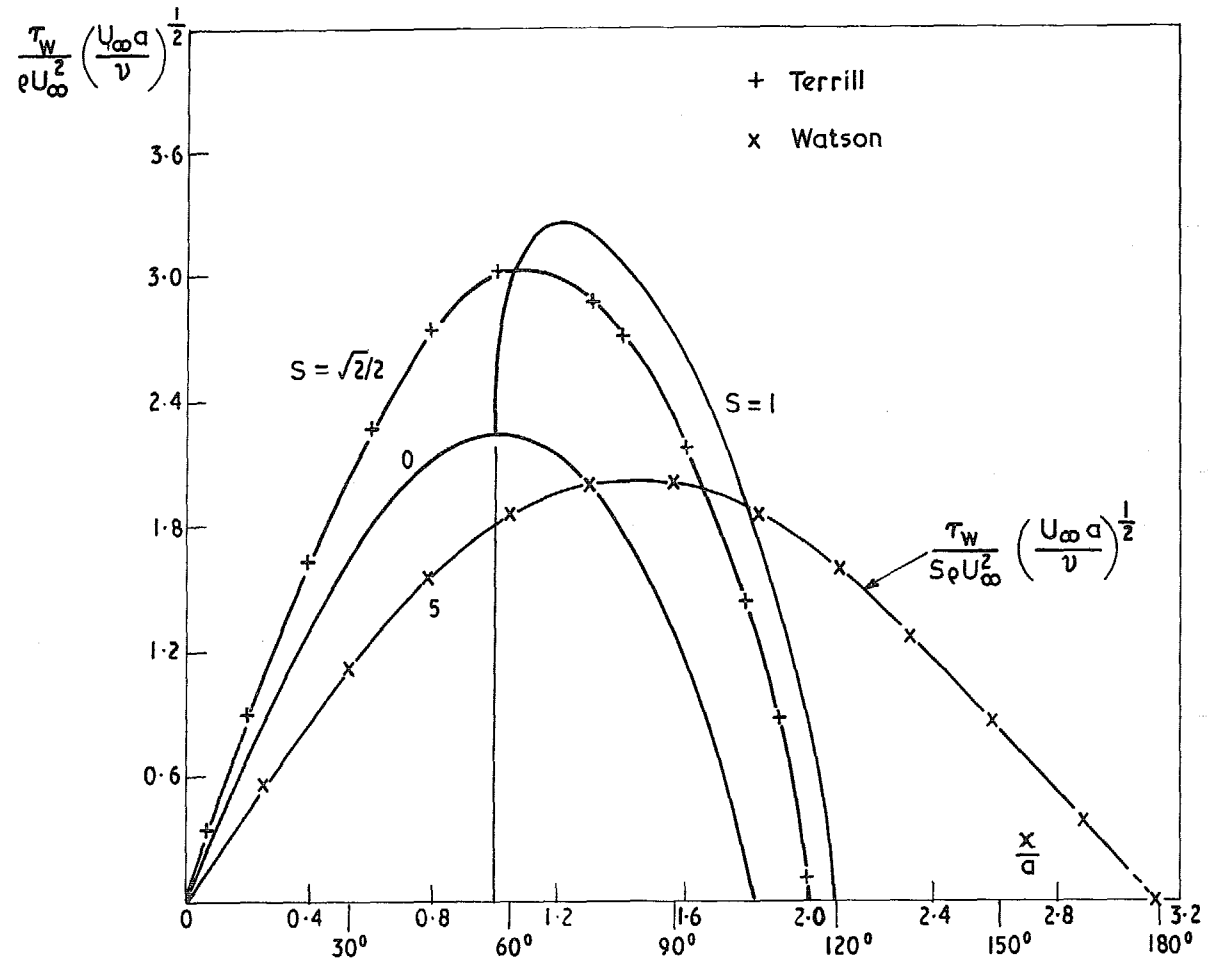
Fig. 9. Circular cylinder $U = 2U_\infty \sin(x/a)$. Shear stress distributions. $S = -(w_0/U_\infty)(U_\infty a/v)^{\frac{1}{2}}$.
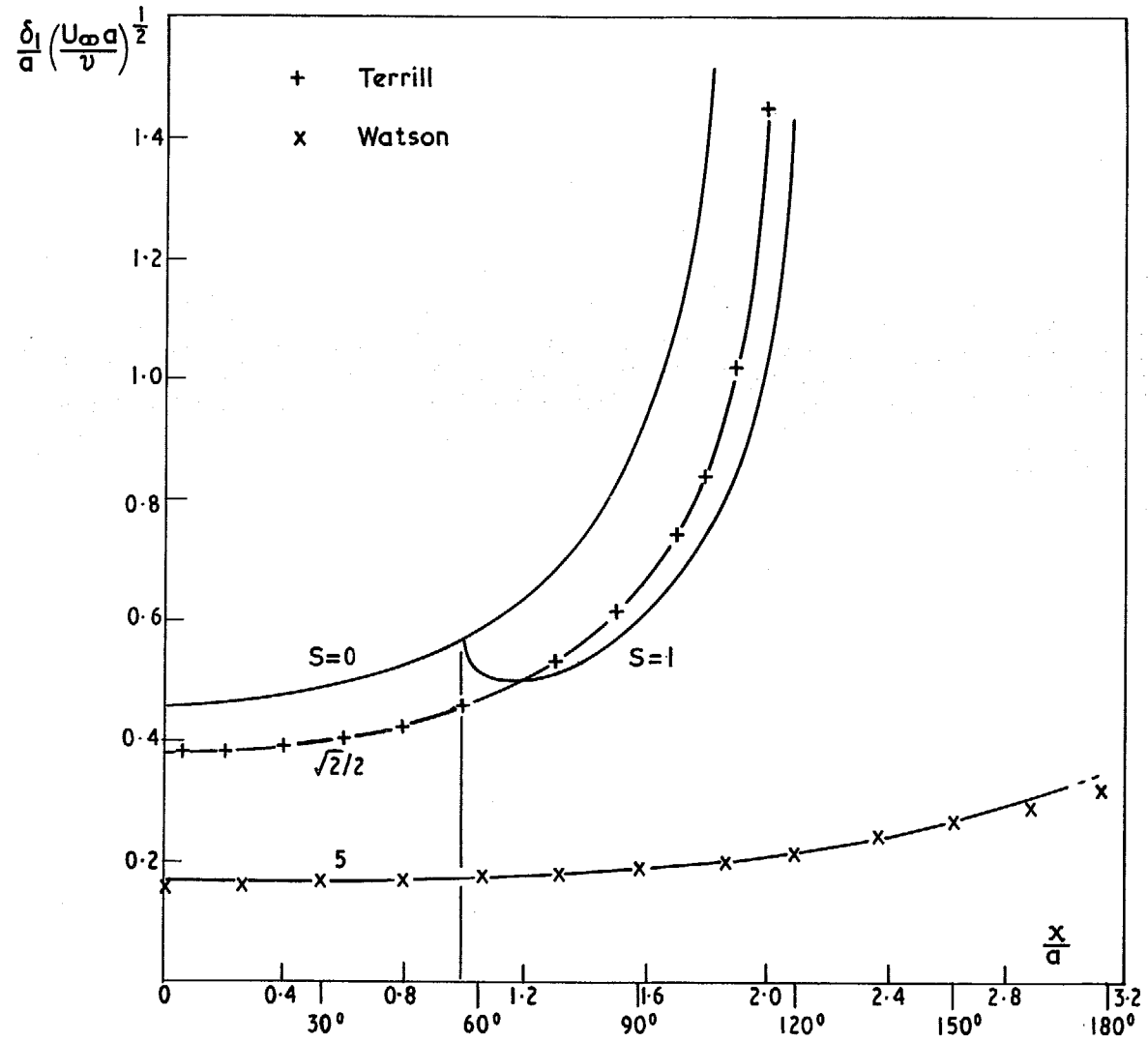
FIG. 10. Circular cylinder $U = 2U_\infty \sin(x/a)$. Displacement thickness distributions.
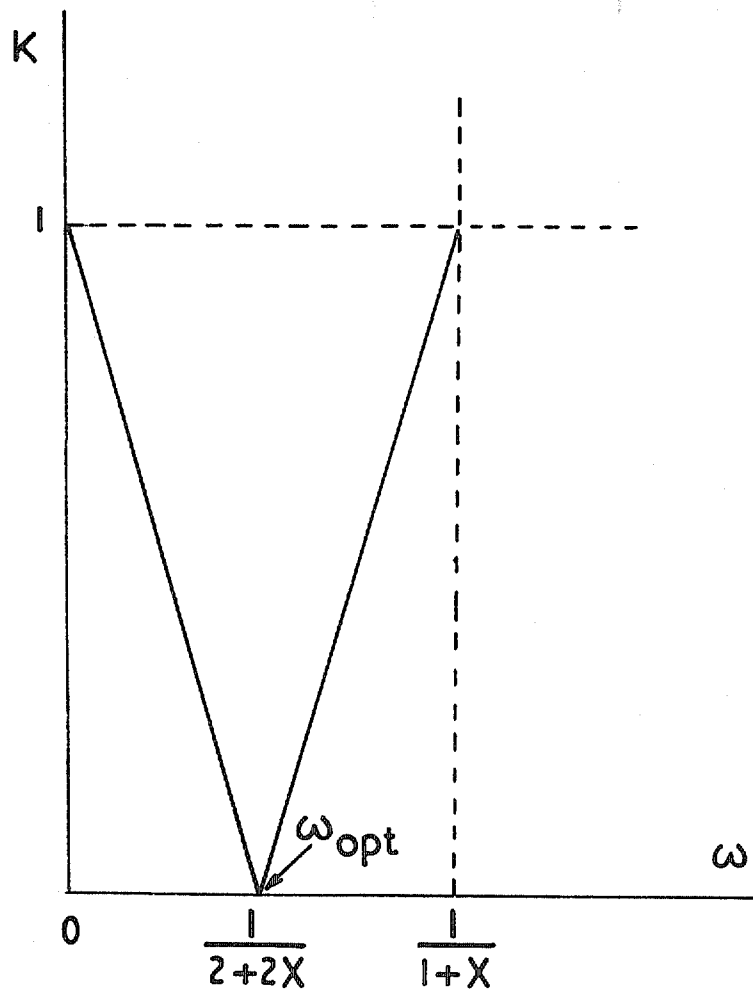
FIG. 11. Simplified problem. Range of convergence of simple iteration process.
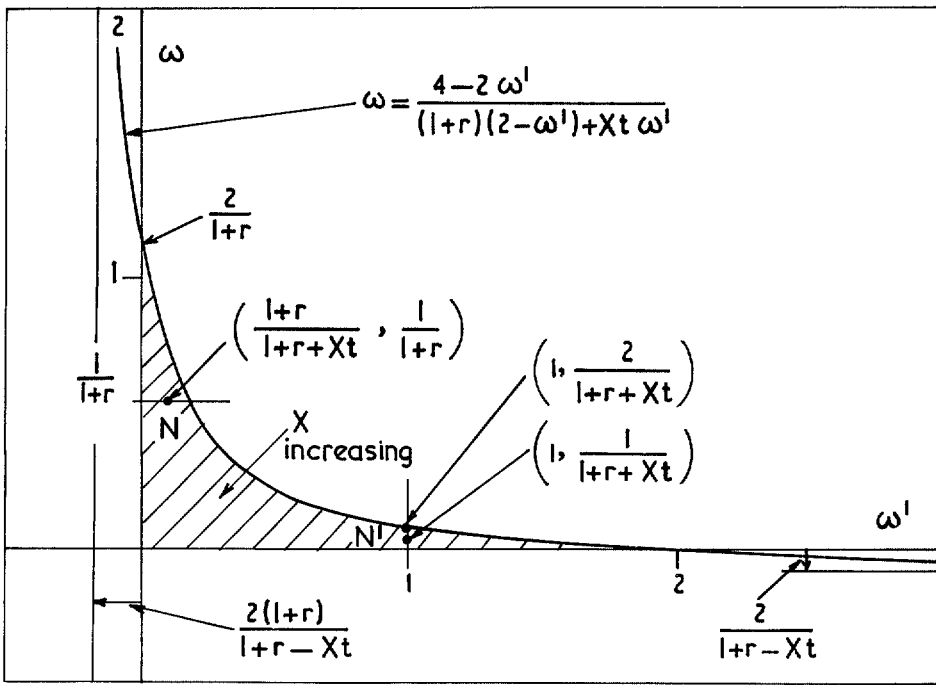
FIG. 12. Simplified problem. Region of convergence of double-field iteration process when $x = 1.0, P = 0.64,$ $G = 0.91, r \approx 0.8$ and $Xt \approx 20.$
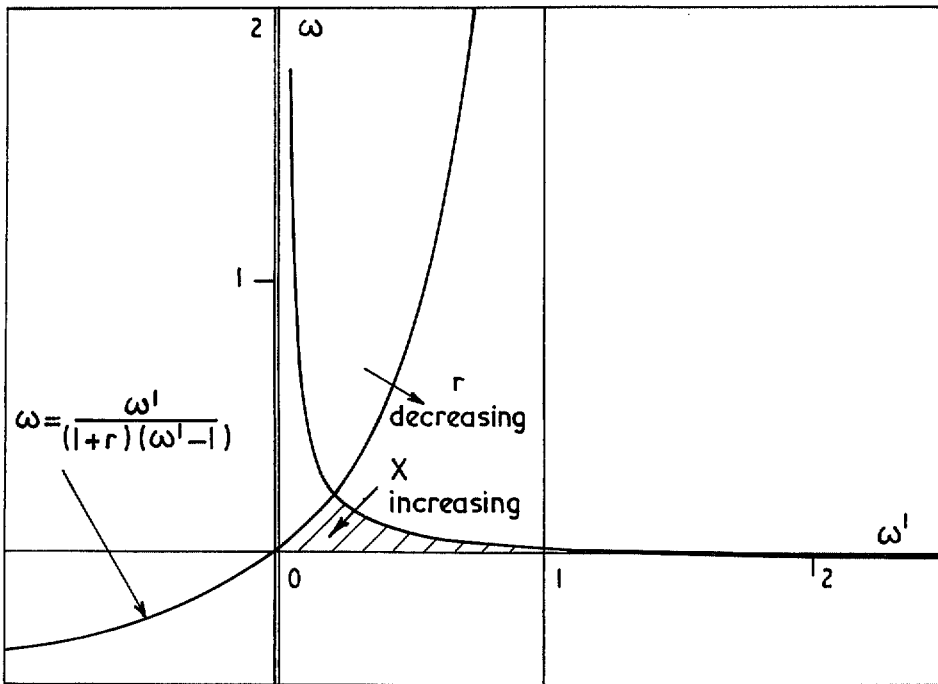
FIG. 13. Simplified problem. Region of convergence of double-field iteration process when $x = 2.0, P = -0.92,$ $G = 0.63, r \approx -2.3, Xt \approx 100.$